Tao A B et al. (2021) EVALUATING SERUM DIA AS A DIAGNOSTIC MARKER FOR ACUTE MYOCARDIAL INFARCTION AND AORTIC DISSECTION IN ATHLETIC PATIENTS. Revista Internacional de Medicina y Ciencias de la Actividad Física y el Deporte vol. 21 (84) pp. 874-917. **DOI:** https://doi.org/10.15366/rimcafd2021.84.015

ORIGINAL

EVALUATING SERUM DIA AS A DIAGNOSTIC MARKER FOR ACUTE MYOCARDIAL INFARCTION AND AORTIC DISSECTION IN ATHLETIC PATIENTS

Ai-Bin Tao[1,2*], Zhen-Wei Mao[3,4#], Zhen-Xiong Jiang[#5], Hao Wang[5], Yong-Wei Yao[5], Bin Lu[2], Dong Zheng

[1]Department of Cardiology, Affiliated People's Hospital of Jiangsu University, Zhenjiang, Jiangsu,212000, China
[2]School of Health and Nursing, Zhenjiang College, Zhenjiang, Jiangsu, China.212000
[3]Center of Laboratory, Affiliated People's Hospital of Jiangsu University, Zhenjiang, Jiangsu, 212000, China
[4]School of Health and Nursing, Zhenjiang College, Zhenjiang, Jiangsu, 212000, China
[5]Department of Cardiology, Affiliated People's Hospital of Jiangsu University, Zhenjiang, Jiangsu,212000, China
E-mail: doctor_aibin@126.com

Recibido 30 de septiembre de 2019 **Received** September 30, 2019
Aceptado 19 de abril de 2019 **Accepted** April 19, 2019

ABSTRACT

Objective: To evaluate the diagnostic potential of serum DIA in detecting differential proteins in athletic patients with aortic dissection (AD) complicated by acute myocardial infarction (AMI). **Methods:** A cohort consisting of AD and AMI patients, including athletes, was assessed from July 2018 to August 2021. Serum DIA levels were compared among 30 participants divided into AD, MI, and control groups. High-throughput DIA quantification and Western blotting were used for protein marker analysis. **Results:** DIA analysis identified significant differences in protein expression among the groups. Proteomic profiling indicated distinct patterns in athletes, with specific markers showing potential for differential diagnosis. The diagnostic value of these markers was further validated using ROC curves. **Conclusion:** The study underscores the diagnostic relevance of serum DIA in athletic patients with AD and AMI, highlighting specific protein markers as potential diagnostic tools. This research contributes to the understanding of cardiovascular risks and diagnostic strategies in athletic populations.

KEYWORDS: DIA; Acute myocardial infarction; Aortic dissection; athletic patient

1. INTRODUCTION

The incidence of aortic dissection (AD) is 7. 2 in 100000 athletic patients, of which 5% are complicated with acute myocardial infarction (AMI). The clinical manifestations of AD complicated with AMI are similar to those of simple AMI, but the treatment plan is contradictory. Therefore, aortic dissection complicated with AMI has a high misdiagnosis rate and mortality (Cui et al., 2021). When ST-T changes or elevated myocardial enzymes are found in electrocardiogram and myocardial enzyme examinations, aortic dissection is easy to be overlooked as the real cause of AMI in clinical diagnosis, and then the wrong treatment is chosen (Hussain et al., 2021). According to a study (Usami, Sai, & Ieda, 2021), thrombolytic treatment significantly increased the mortality of individuals with aortic dissection compared to non-misdiagnosed athletic patients (55.6% vs. 21.2%). In recent years, the incidence of AMI in aortic dissection is increasing, but the number of reported cases is limited. The incidence ratio of male to female is 2:1, and the age of onset is relatively young. About 75% of athletic patients with aortic dissection are complicated with hypertension, Marfan syndrome and other risk factors (Chen, Lu, & Sung, 2019). Aortic dissection describes the creation of true and false lumens in the aorta as a result of blood entering the aortic media from the aortic intima tear and expanding and peeling along the long axis of the aorta (Zhang, Yang, & Wang, 2021). AMI can be complicated when the coronary artery opening or branch is involved in the retrograde progression of aortic dissection (F. Liu et al., 2021).

Standford classifies the dissection according to whether it involves the ascending aorta: dissection involving the ascending aorta is type A, while dissection without ascending aorta is type B (Wang, Wu, Zhao, You, & Li, 2019). Most of the aortic dissection complicated with AMI is type A aortic dissection. Clinically, the timely diagnosis and correct treatment of aortic dissection complicated with AMI are very important. The study of proteomics investigates how proteins in cells, organs, and living things change with time (Li, Gonzalez-Lozano, Koopmans, & Smit, 2020). In order to fully comprehend the relationship between the occurrence of diseases and cell metabolism and other processes from the protein level, the field of proteomics refers to the study of the characteristics of proteins on a large scale, including the expression level of proteins, post-translational modifications, protein-protein interactions (Quan et al., 2021). In the past twenty years, mass spectrometry (MS) has become the preferred method, has been widely used in the quantitative detection of proteins in biological samples (Karayel, Michaelis, Mann, Schulman, & Langlois, 2020), the method has the advantages of high reliability and wide applicability, greatly promote the understanding and the understanding of cellular signal transduction network, help to clarify protein interactions in different cell state, It is conducive to understanding the disease mechanism and promoting the level of disease diagnosis (Farmer, Rushmer, Wykes, & Mallmann, 2020). Therefore, this study collected athletic patient's serum samples, through the DIA

technology is used to detect the omics analysis, screening of protein markers and experiment validation, looking for high specificity and sensitivity of the protein markers, and explore relevant molecular pathways, clear differences in protein value to the diagnosis of aortic dissection and AMI, provides ideas for its diagnosis.

2. Data and research methods

2.1 General Information of Subjects

From July 2018 to August 2021, 10 athletic patients with AD complicated with AMI and 10 subjects with simple AMI in our hospital were collected, and 10 normal physical examinations were selected. The study enrolled 30 participants who were meticulously divided into three groups: AD, MI, and Sham. Each group comprised five individuals for both serum DIA detection and Western blot analysis. This balanced design ensured adequate representation of each group and allowed for robust comparisons between the detection methods and across the different participant categories. Additionally, the utilization of two different detection methods, serum DIA and Western blot, provided valuable insights into the potential variations in protein expression and activity across the groups. This multifaceted approach strengthened the study's findings and enhanced its overall significance.

The inclusion criteria of subjects in the AD group are shown as follows: AD combined with AMI confirmed by aortic CT angiography; On admission, blood samples were drawn to detect serum DIA or Western blot. Exclusion criteria of AD group (König et al., 2021): The subject has a history of thrombotic disease; Malignant tumor, atrial fibrillation, severe liver disease, etc. Inclusion criteria in MI group: acute myocardial infarction confirmed by coronary angiography; On admission, blood samples were drawn to detect serum DIA or Western blot.

Exclusion criteria for MI group (Zlatanovic et al., 2021): malignant tumor, atrial fibrillation, severe liver disease, etc. The inclusion criteria of normal physical examination in the Sham group were: The subjects were between 18 and 80 years old; Blood was drawn to detect serum DIA or Western blot; The physical examination results were basically normal. Exclusion criteria for normal physical examination in Sham group: athletic patients with cardiovascular disease. The study was conducted after review and approval by our hospital ethics committee.

2.2 methods

2.2.1 How blood samples are collected and stored

Blood was collected from the subjects and placed in a separating gel

tube, centrifuged at low temperature immediately, and the upper serum was collected into the sterile centrifuge tube and stored in the refrigerator at -80℃. General information and serum DIA test results were obtained by retrospective review of medical records.

2.2.2 DIA experiment method

2.2.2.1 Reagent

Sodium dodecyl sulfate (SDS) was purchased from Beijing Solibao Technology Co., LTD. Ammonium bicarbonate (NH4HCO3) was purchased from Jiangsu Tianjingsha Gene Diagnosis Technology Co., LTD. Trifluoroacetic acid (TFA) was purchased from Shanghai Aladdin Biochemical Technology Co., LTD. Dithiothreitol (DTT) was purchased from Hubei Hanwei Chemical Co., LTD. Iodoacetamide (IAA) was purchased from Wuhan Ximoment Biotechnology Co., LTD.

Tris-HCI was purchased from Qingdao Kester Biotechnology Co., LTD. Lysyl peptide endonuclease (LysC) Beijing Norblad Technology Co., LTD. Trypsin was purchased from Shanghai Jingkang Bioengineering Co., LTD. SOLAμHRP desalted 96-well plates were purchased from ThermoScientific. Mass spectrometry grade methanol and acetonitrile were purchased from Fisher Scientific, and ultrapure water (ddH2O) was prepared by a laboratory pure water mechanism (Thermo Scientific).

2.2.2.2 Preparation of mass spectrometry protein samples

After the protein level was determined by BCA method, 50 μg protein was taken and 6 mol/L urea was added for 30 reactions. Then iodoacetamide was added to control the level of 6.25 mmol/L, and the reaction was kept away from light for 1 h. Ammonium bicarbonate was added to dilute the reaction and then human calcium chloride was added for 1 mmol/L. Pancreatic enzymes were denatured in alkaline environment, and the reaction was carried out at 37 C for 16 h.

2.2.2.3 Mass spectrometry data collection

The EASY nLC-1000 UP-LC system combined with Orbitrap mass spectrometer Q Exactive plus mass spectrometer was used for data acquisition with 1 μg sample load on the same homemade C18 column. Separation phase: A phase was 0.1% formic acid, B phase was 0.1% formic acid plus 80% acetonitrile, ambient temperature was controlled at 4 °C.

Gradient elution procedure: 0-5 min, 97%-93% of phase A, 3%-7% of phase B; > 5~ 55min, A phase 93%-78%,B phase 7%-22%; > 55-65 min, phase A 78%-65%, phase B 22%-35%; > 65~68 min, phase A 65%~ 20%, phase B

35%~80%; >68~75 min, phase A 20%, phase B 80%.

2.2.2.4 Mass spectrometry method

DDA scanning: Positive ion scanning was used, the range was 400~1 200 m/z, and the time was 75 min. The first-stage scan mode is full scan, the range is 400~1 200 m/z, and the first-stage detection orbit resolution is 70 000 FWHM@200 m/z. Automatic gain control was 3X10°, maximum ion injection time was 50 ms, charge number 2-7, loopcount 20, secondary mass spectrometry fragmentation mode HCD, collision energy NCE was 27%, secondary automatic gain control was 5X10. DIA data acquisition: the first-level scan mode is full scan, the range is 400~1 200 m/z, the first-level detection orbit resolution is 35 000 FWHM@200 m/z, the AGC is 5×105, and the window is 32 fixed Windows, each window is to select, fragment, collect parent ion information and all daughter ion information for quantification.

2.2.2.5 Data and biological information analysis

The DDA data were searched by Proteome Discoverer software, and the results were imported into Sky-line software for database construction and data analysis and extraction.

2.2.2.6 Functional analysis of differential proteins

Protein import will be increased and downgrade webgestalt (http://www.webgestalt.org/) on the GO, KEGG functional annotation, enrichment of analysis, screening of FDR < 0.05 GO and KEGG enrichment.

2.2.2.7 Clinical validation of potential markers

2.2.2.7.1 Western blot

Serum samples were obtained, lysed, and protein was extracted. BCA method was used to determine the concentration of total protein, and the loading amount was determined. Sds-page gels were prepared, electrophoretic, transmembrane, and blocked with 5% nonfat milk powder protein. The primary antibody was added and incubated at 4℃ overnight, and the secondary antibody (rat anti-rabbit 1:200) was incubated at 37℃ for 1h, then washed with TBST and developed.

2.3 Observation Indicators

The differential protein, protein function and enrichment analysis were observed in the serum DIA detection group, and the relative expression of differential protein was verified by Western blot, so as to clarify the diagnostic value of differential protein in AD complicated with AMI.

2.4 Statistical Methods

DIA data was imported into Spectronaut 14 with FDR<1% for both peptide and protein expression levels. Spectronaut was used to calculate the normalized Protein intensity.

The average value of Top3 peptides calculated by Spectronaut was the Protein intensity, and the median normalization method was used to normalize Protein intensity. For statistical analysis, the protein intensity was exported into Perseus and Metaboanalyst. Before statistical analysis, Log2 transformation was performed on the original data.

The detection values containing at least 60% in any group were used as variable filtering criteria, and KNN Sample-wise missing values were filled in. P-value <0. 05 was set as the screening condition for differential proteins. In SIMCA-P software, principal component analysis (PCA) and OPLS-DA were carried out. Graphing with the GraphPad Prism program; the receiver operating characteristic curve was created using SPSS software after data analysis (ROC).

Calculations were made to determine the curve's sensitivity, specificity, and area under the curve (AUC). Binary logistic regression analysis was performed on the combined detection data to obtain the predicted value of protein detection probability, which was used to draw the ROC curve. P<0.05 was considered statistically significant.

3 Results

3.1 DIA technique to detect differential proteins

In this experiment, the label-free quantitative protein value omics DIA technology was used to analyze serum samples. After removing the peak protein, the digested peptide was analyzed by liquid mass spectrometry.

The FDR of peptide and protein was strictly controlled to be less than 1%, and 1063 proteins were quantified in 15 samples. Nearly 900 proteins were quantified in each sample (except for M/2 and sample 4, from Zhenjiang). Fig. 1), and the dynamic intensity ranges of these proteins exceeded six orders of magnitude (Fig.2).

After missing values were processed in accordance with the following rules, the obtained data set was used for project data mining :(1) Protein molecules with missing values greater than 40% in any group were eliminated (that is, missing values were found in more than 2 samples out of 5 samples in each group); (2) KNN algorithm (sample-wise) was used to fill in the data sets filtered by missing values; (3) After processing, 769 proteins were used for

statistical analysis.

PCA was used to perform logarithmic transformation and Pareto proportional modeling on DIA proteomic data, and the model parameter was R2X=0.349, indicating significant differences in the expression of several histones (Fig. 3).

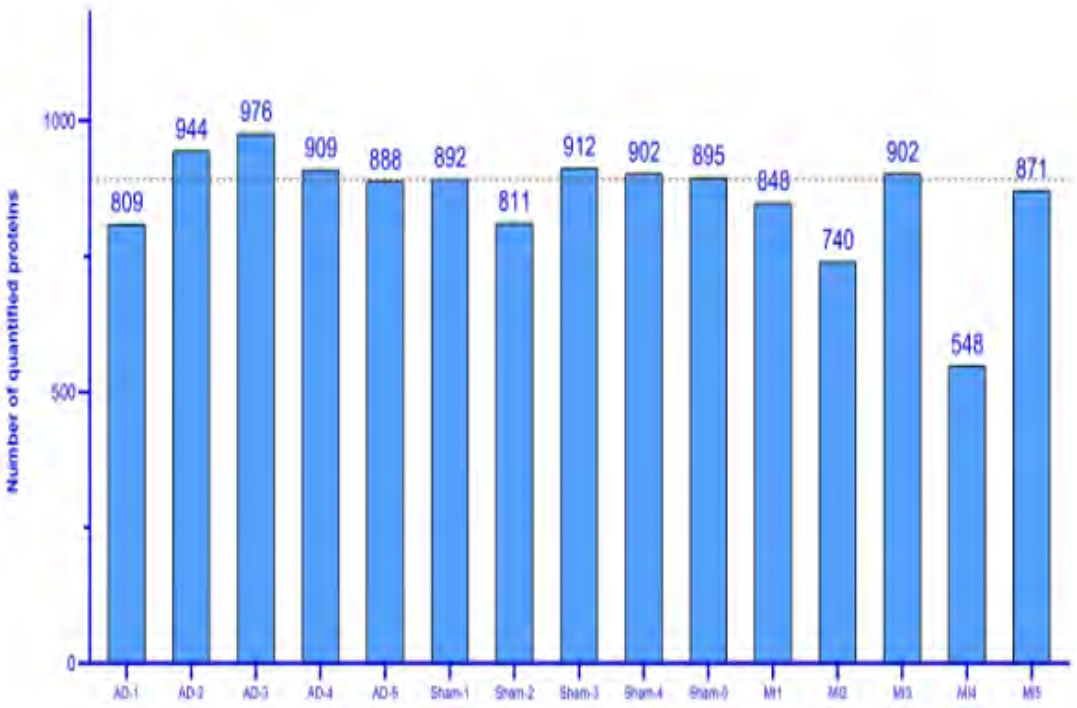

Figure 1: Number of proteins that DIA-MS measured for each sample group

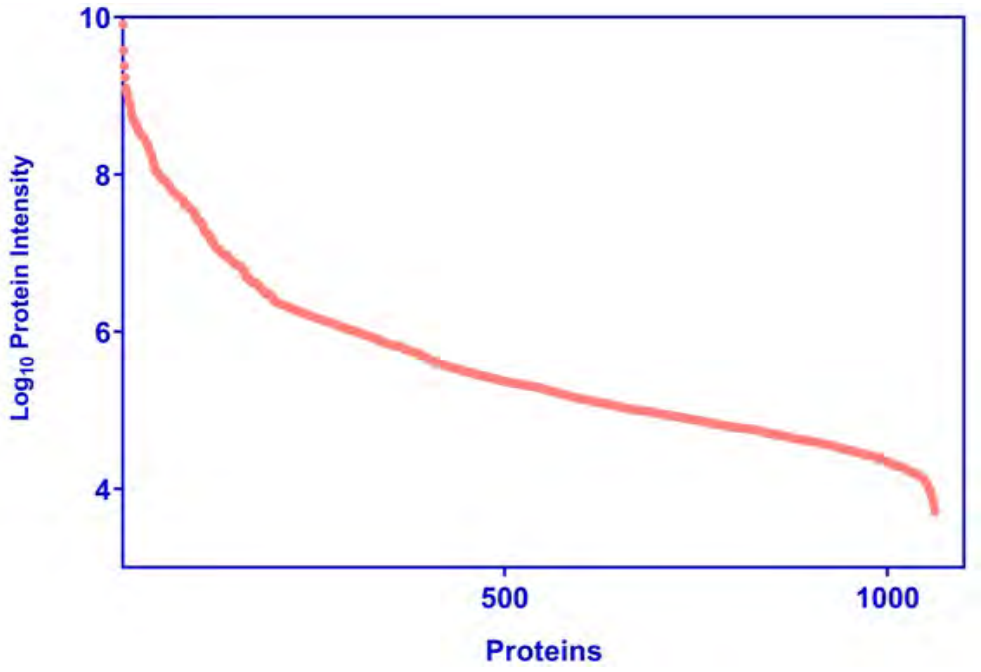

Figure 2: All quantified proteins' dynamic range. X-coordinates and Y-Log10 intensities

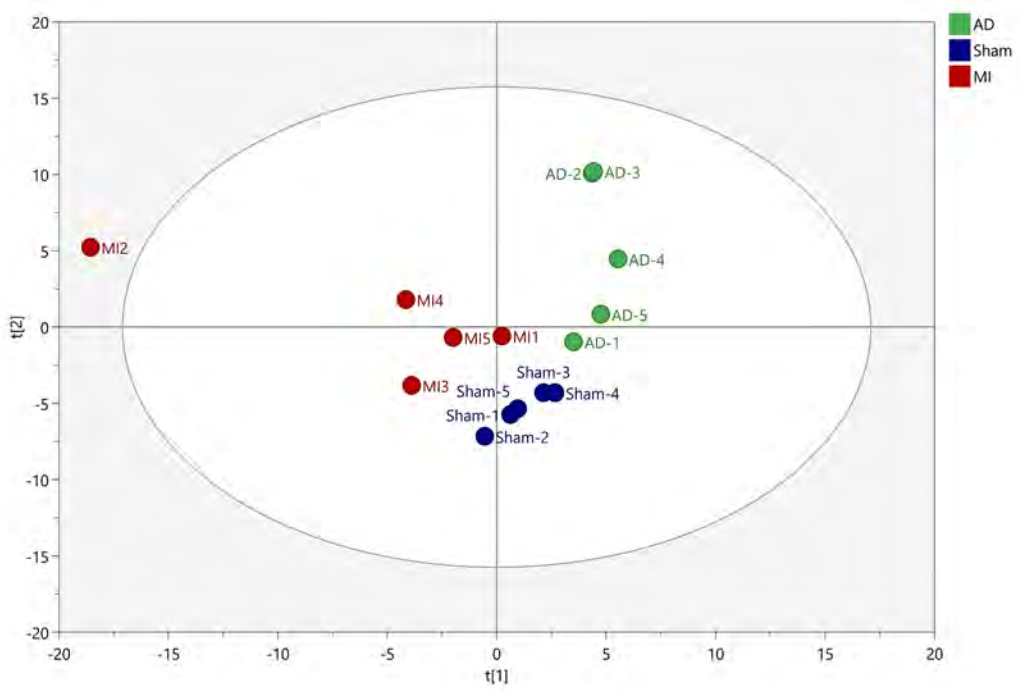

Figure 3: Plots of metabolic phenotypes using unsupervised PCA scores comparing the MI, AD, and Sham groups. For modeling, DIA proteomic data was log transformed and pareto scaled. Model specification: R2X=0.349 (cumulative variance proportion of 2 principal components).

3.2 Comparison between MIvsSham groups

3.2.1 Principal component analysis results of MI group vsSham group

The two groups showed a certain classification trend in PCA diagram, and the surface proteome changed between the two groups (Fig.4). Individual differences were significant in the MI group.

In the sample cluster dispersion analysis, the Score Plot of Principal Component Analysis (PCA) plays a crucial role. This plot utilizes the first two or three principal components, which are essentially projections of the original multidimensional data onto a lower-dimensional space.

These components capture the most significant variations within the data, facilitating visualization and interpretation of complex relationships. The X and Y axes of the Score Plot represent the first principal component (T1) and the second principal component (T2), respectively.

By examining the relative positions of different data points in this reduced-dimensional space, researchers can identify clusters, outliers, and trends within the sample population. This valuable tool allows for a deeper understanding of the underlying structure and relationships present within the data, ultimately leading to more informed conclusions and meaningful insights.

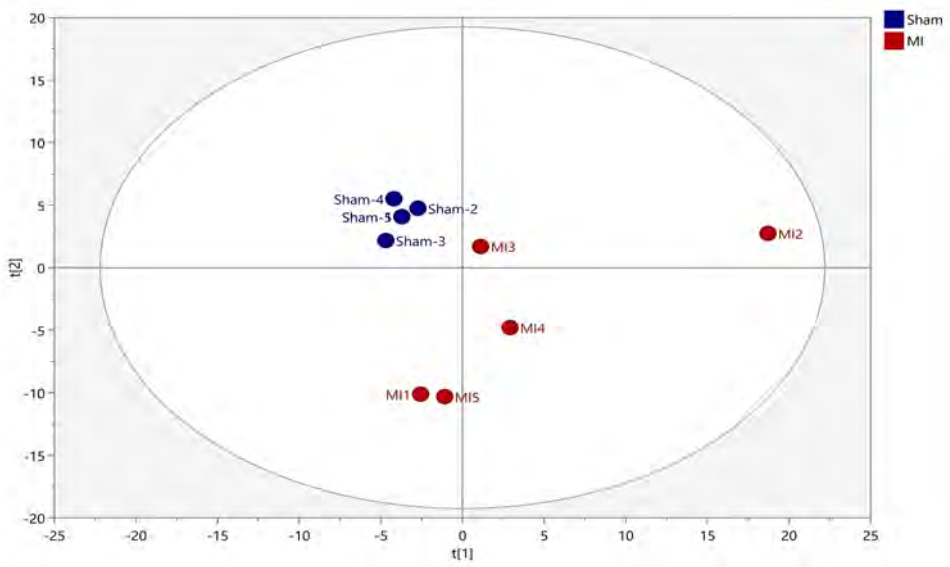

Figure 4: Metabolic phenotype unsupervised PCA score graphs between the MI and Sham groups. For modeling, DIA proteomic data was log transformed and pareto scaled. Model specification: R2X=0 471 (cumulative variance proportion of 2 principal components).

3.2.2 Results of a discriminant analysis using orthogonal partial least squares between the MIvsSham groupings

The two groups' proteomic data were significantly different, as shown by PCA, Q2 > 0.5, and the model performed well in terms of prediction (Fig.5). The robustness of the OPLS-DA model was tested using 100 times of displacement after the S-plot was used to filter the metabolites with high correlation of the primary components (Fig.6). The intercepts of Q2 of the model was -0.123 and the slope was positive, indicating that the model was robust (Fig.7).

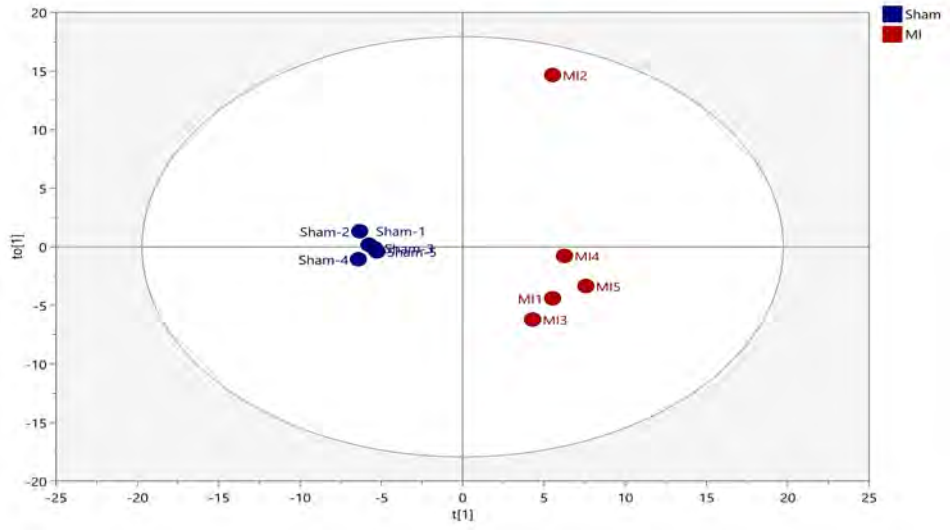

Figure 5: To optimize inter-group distinction of metabolomic data between the MI and Sham groups, a score plot of OPL S-DA modeling was created. Model specification: R2Y=0.98, Q2=0.736, 1 orthogonal + 1 predictive component.

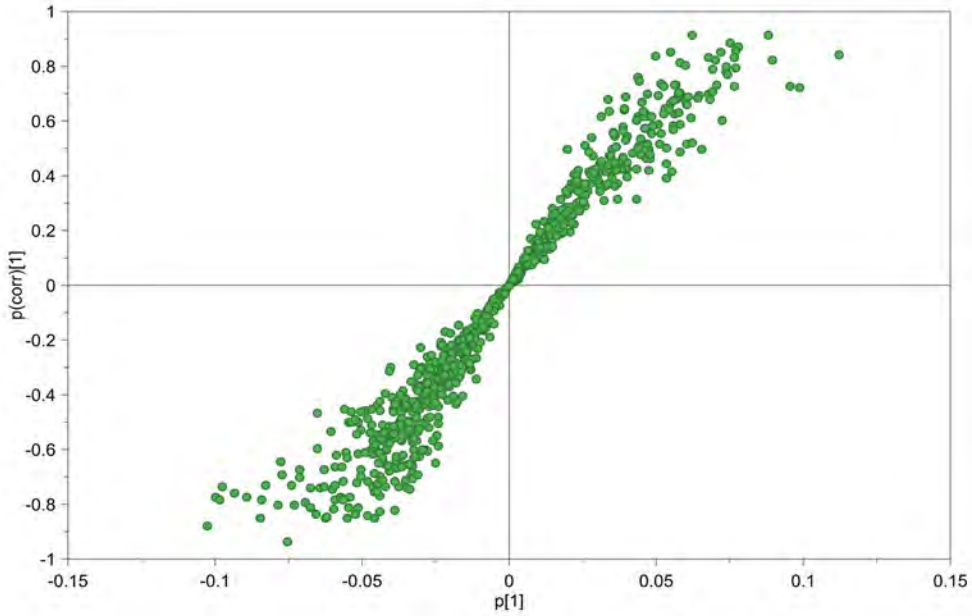

Figure 6: S-plot of OPLS-DA model between MI and Sham groups.

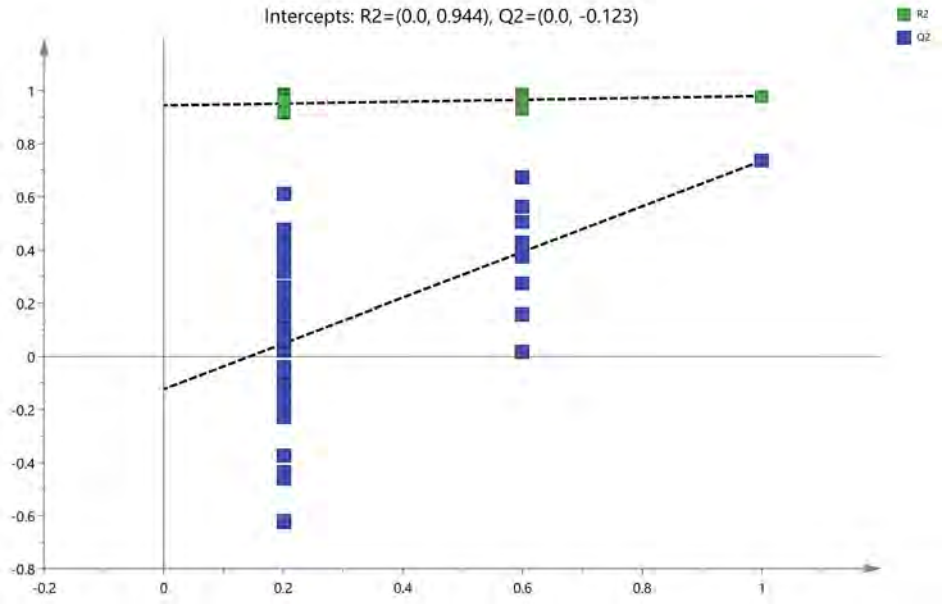

Figure 7: 100 times permutation to test robustness of OPl S-DA modeling.

3.2.3 Differential protein screening between MI vs Sham groups

The differentially expressed proteins between the two groups were screened with P 0.05 as the cutoff, and the quantitative protein data of the MI group and Sham group were compared using a t-test. 137 proteins were discovered to be differently expressed when the original P-value was utilized to identify them, with 55 of the proteins showing up-regulation (MI/Sham). Eighty-two proteins were down-regulated (Fig. 8). Detailed differential protein information is shown in Tab. 1 and Tab. 2.

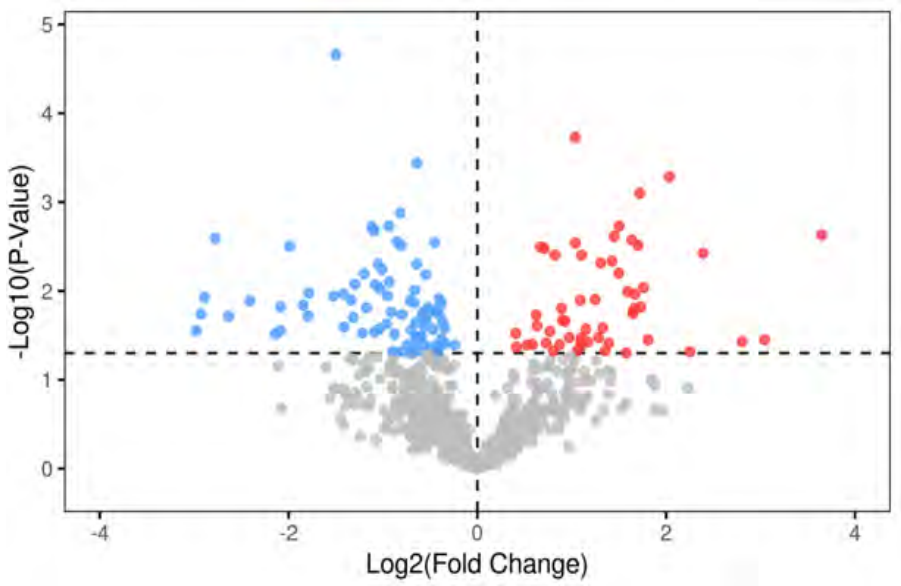

Figure 8 Visualizing MI and Sham using a volcano map of quantitative DIA proteomics data. Proteins that had a significance level of p0.05 were highlighted in red. Each volcano plot showed the number of proteins that were up-regulated and those that were down-regulated.

Table 1(a) Up-expressed protein in MI in comparison to Sham **(**p<0.05**)**

UNIPROT ID	PROTEIN.DESCRIPTION	P-VALUE	FOLD CHANGE
P09211	GLUTATHIONE S-TRANSFERASE P	0.00234297	12.53056713
P02679	FIBRINOGEN GAMMA CHAIN	0.03546928	8.24182263
P02675	FIBRINOGEN BETA CHAIN	0.03723935	6.98838284
P60174	TRIOSEPHOSPHATE ISOMERASE	0.00377143	5.24894653
P40925	MALATE DEHYDROGENASE, CYTOPLASMIC	0.04817824	4.76140122
P80748	IG LAMBDA CHAIN V-III REGION LOI	0.00051929	4.09643346
P08519	APOLIPOPROTEIN(A)	0.03557482	3.50606768
B9A064	IMMUNOGLOBULIN LAMBDA-LIKE POLYPEPTIDE 5	0.00916502	3.38561586
P06744	GLUCOSE-6-PHOSPHATE ISOMERASE	0.01512355	3.32058206
P10153	NON-SECRETORY RIBONUCLEASE	0.00079622	3.29441009
P00558	PHOSPHOGLYCERATE KINASE 1	0.00307096	3.25671799
P35579	MYOSIN-9	0.01084143	3.1778594
O95897	NOELIN-2	0.0155599	3.17583155
Q9BYE9	CADHERIN-RELATED FAMILY MEMBER 2	0.01694095	3.14391775
P08833	INSULIN-LIKE GROWTH FACTOR-BINDING PROTEIN 1	0.01793199	3.13609788
P01717	IG LAMBDA CHAIN V-IV REGION HIL	0.00266345	3.1063578

Table 1(b) Up-expressed protein in MI in comparison to Sham (p<0.05)

Q01518	ADENYLYL CYCLASE-ASSOCIATED PROTEIN 1	0.01017029	3.01175401
P62807	HISTONE H2B TYPE 1-C/E/F/G/I	0.04986037	2.98265299
Q96NZ9	PROLINE-RICH ACIDIC PROTEIN 1	0.00186499	2.83041507
P61981	14-3-3 PROTEIN GAMMA	0.00631819	2.82316758
P18669	PHOSPHOGLYCERATE MUTASE 1	0.00243943	2.73072497
P0DMV8;P0DMV9	HEAT SHOCK 70 KDA PROTEIN 1A	0.00461746	2.68811898
P07988	PULMONARY SURFACTANT-ASSOCIATED PROTEIN B	0.03878543	2.62471586
P62736;P63267	ACTIN, AORTIC SMOOTH MUSCLE	0.0469968	2.55641683
P00995	SERINE PROTEASE INHIBITOR KAZAL-TYPE 1	0.02596889	2.50923851
Q6Q788	APOLIPOPROTEIN A-V	0.00484304	2.4731537
P01714	IG LAMBDA CHAIN V-III REGION SH	0.03348487	2.43414189
P00451	COAGULATION FACTOR VIII	0.01248055	2.37546056
P78417	GLUTATHIONE S-TRANSFERASE OMEGA-1	0.03749339	2.24724904
P07108	ACYL-COA-BINDING PROTEIN	0.02685899	2.21900567
P05154	PLASMA SERINE PROTEASE INHIBITOR	0.003958	2.15087136
P01861	IG GAMMA-4 CHAIN C REGION	0.03348919	2.14368421
Q13188	SERINE/THREONINE-PROTEIN KINASE 3	0.03803868	2.1386372
P01833	POLYMERIC IMMUNOGLOBULIN RECEPTOR	0.0422721	2.13267344
P14618	PYRUVATE KINASE PKM	0.01274478	2.12833213
P31146	CORONIN-1A	0.04701937	2.08003052
Q99536	SYNAPTIC VESICLE MEMBRANE PROTEIN VAT-1 HOMOLOG	0.0028795	2.05450011
P03951	COAGULATION FACTOR XI	0.00018657	2.05095629
Q86UX7	FERMITIN FAMILY HOMOLOG 3	0.03343492	1.96329992
O75083	WD REPEAT-CONTAINING PROTEIN 1	0.02201079	1.90591977
P0CG05	IG LAMBDA-2 CHAIN C REGIONS	0.02116293	1.8664591
P61916	EPIDIDYMAL SECRETORY PROTEIN E1	0.01563359	1.85435605
P30740	LEUKOCYTE ELASTASE INHIBITOR	0.04011783	1.82838943
P02787	SEROTRANSFERRIN	0.00394417	1.76737835
P05090	APOLIPOPROTEIN D	0.04735337	1.74623635
Q9ULI3	PROTEIN HEG HOMOLOG 1	0.02850217	1.70418241
P02792	FERRITIN LIGHT CHAIN	0.03853469	1.65654878
Q8IYS5	OSTEOCLAST-ASSOCIATED IMMUNOGLOBULIN-LIKE RECEPTOR	0.00332567	1.63701316

Table 1(c) Up-expressed protein in MI in comparison to Sham (p<0.05)

Q13643	FOUR AND A HALF LIM DOMAINS PROTEIN 3	0.00318624	1.58888278
P46531	NEUROGENIC LOCUS NOTCH HOMOLOG PROTEIN 1	0.02476435	1.55158569
Q92736	RYANODINE RECEPTOR 2	0.01869407	1.53989604
Q92954	PROTEOGLYCAN 4	0.03993748	1.49981621
P13489	RIBONUCLEASE INHIBITOR	0.04059781	1.4385492
P11279	LYSOSOME-ASSOCIATED MEMBRANE GLYCOPROTEIN 1	0.04291764	1.33188701
Q9BXR6	COMPLEMENT FACTOR H-RELATED PROTEIN 5	0.03008046	1.32553304

Table 2(a) Down-expressed protein in MI in comparison to Sham (p<0.05)

UNIPROT ID	PROTEIN.DESCRIPTION	P-VALUE	FOLD CHANGE
P07357	COMPLEMENT COMPONENT C8 ALPHA CHAIN	0.04056129	0.84779195
P02652	APOLIPOPROTEIN A-II	0.03887349	0.79102531
Q13822	ECTONUCLEOTIDE PYROPHOSPHATASE/PHOSPHODIESTERASE FAMILY MEMBER 2	0.02623804	0.78750842
P08195	4F2 CELL-SURFACE ANTIGEN HEAVY CHAIN	0.02229397	0.77431436
P15169	CARBOXYPEPTIDASE N CATALYTIC CHAIN	0.01392897	0.76984926
P07358	COMPLEMENT COMPONENT C8 BETA CHAIN	0.03451044	0.76827386
P10909	CLUSTERIN	0.04169065	0.76262866
P05156	COMPLEMENT FACTOR I	0.01860624	0.7562657
P02765	ALPHA-2-HS-GLYCOPROTEIN	0.01227802	0.75508892
Q12913	RECEPTOR-TYPE TYROSINE-PROTEIN PHOSPHATASE ETA	0.0497411	0.74883319
P08253	72 KDA TYPE IV COLLAGENASE	0.04068173	0.74258026
P22352	GLUTATHIONE PEROXIDASE 3	0.01640238	0.7400065
P13671	COMPLEMENT COMPONENT C6	0.00286002	0.73118859
P15144	AMINOPEPTIDASE N	0.01665914	0.72678622
Q9NRN5	OLFACTOMEDIN-LIKE PROTEIN 3	0.0270816	0.72274905
P28906	HEMATOPOIETIC PROGENITOR CELL ANTIGEN CD34	0.04330911	0.70513727
Q16610	EXTRACELLULAR MATRIX PROTEIN 1	0.04983856	0.697339
Q14515	SPARC-LIKE PROTEIN 1	0.01533808	0.69448459
P49908	SELENOPROTEIN P	0.02078211	0.69022224

Table 2(b) Down-expressed protein in MI in comparison to Sham (p<0.05)

P04217	ALPHA-1B-GLYCOPROTEIN	0.00655966	0.6845143
P19823	INTER-ALPHA-TRYPSIN INHIBITOR HEAVY CHAIN H2	0.02547568	0.67801187
P06396	GELSOLIN	0.03986918	0.67309182
P07359	PLATELET GLYCOPROTEIN IB ALPHA CHAIN	0.01738115	0.66985618
P27797	CALRETICULIN	0.01977801	0.66935685
P20851	C4B-BINDING PROTEIN BETA CHAIN	0.03299406	0.66342381
P09871	COMPLEMENT C1S SUBCOMPONENT	0.03248567	0.66143025
Q9H4A9	DIPEPTIDASE 2	0.03252228	0.65542603
P36955	PIGMENT EPITHELIUM-DERIVED FACTOR	0.03694449	0.64147304
Q96KN2	BETA-ALA-HIS DIPEPTIDASE	0.00036499	0.64130818
P24592	INSULIN-LIKE GROWTH FACTOR-BINDING PROTEIN 6	0.00498173	0.6407294
O94985	CALSYNTENIN-1	0.04762901	0.63932763
O00451	GDNF FAMILY RECEPTOR ALPHA-2	0.0326583	0.63721381
P13591	NEURAL CELL ADHESION MOLECULE 1	0.02260629	0.63408366
P43251	BIOTINIDASE	0.00978925	0.63200075
Q86WI1	FIBROCYSTIN-L	0.01355229	0.62876263
O94769	EXTRACELLULAR MATRIX PROTEIN 2	0.02764572	0.61554712
P00533	EPIDERMAL GROWTH FACTOR RECEPTOR	0.01279524	0.6104931
Q86TY3	UNCHARACTERIZED PROTEIN C14ORF37	0.0498502	0.60986526
P19021	PEPTIDYL-GLYCINE ALPHA-AMIDATING MONOOXYGENASE	0.04048541	0.59940793
Q8IWV2	CONTACTIN-4	0.01844551	0.57491217
P01024	COMPLEMENT C3	0.04779723	0.5748903
Q8IUL8	CARTILAGE INTERMEDIATE LAYER PROTEIN 2	0.00306482	0.57150233
Q10471	POLYPEPTIDE N-ACETYLGALACTOSAMINYLTRANSFERASE 2	0.00133078	0.56725788
P14151	L-SELECTIN	0.00280976	0.55444158
Q15166	SERUM PARAOXONASE/LACTONASE 3	0.03072559	0.54381035
P00736	COMPLEMENT C1R SUBCOMPONENT	0.04813779	0.53622565
P24593	INSULIN-LIKE GROWTH FACTOR-BINDING PROTEIN 5	0.01739817	0.53107553
P11597	CHOLESTERYL ESTER TRANSFER PROTEIN	0.00786777	0.52365581
Q76LX8	A DISINTEGRIN AND METALLOPROTEINASE WITH THROMBOSPONDIN MOTIFS 13	0.0018595	0.52225175

Table 2(c) Down-expressed protein in MI in comparison to Sham (p<0.05)

P49641	ALPHA-MANNOSIDASE 2X	0.01126831	0.51681836
Q9NQ38	SERINE PROTEASE INHIBITOR KAZAL-TYPE 5	0.02358898	0.5133237
Q16706	ALPHA-MANNOSIDASE 2	0.00571695	0.4958269
P34096	RIBONUCLEASE 4	0.00954359	0.48970128
Q15828	CYSTATIN-M	0.02698601	0.48560084
O43505	BETA-1,4-GLUCURONYLTRANSFERASE 1	0.00497178	0.48236896
P02766	TRANSTHYRETIN	0.00854414	0.47232127
P01033	METALLOPROTEINASE INHIBITOR 1	0.02897818	0.46947755
P22105	TENASCIN-X	0.00209298	0.46825439
P02768	SERUM ALBUMIN	0.00189804	0.46013012
P08185	CORTICOSTEROID-BINDING GLOBULIN	0.01543974	0.44308189
P14543	NIDOGEN-1	0.00642621	0.43537951
Q07075	GLUTAMYL AMINOPEPTIDASE	0.02981932	0.43009363
Q96S96	PHOSPHATIDYLETHANOLAMINE-BINDING PROTEIN 4	0.00841906	0.40662044
Q9Y274	TYPE 2 LACTOSAMINE ALPHA-2,3-SIALYLTRANSFERASE	0.01987895	0.4019432
P27169	SERUM PARAOXONASE/ARYLESTERASE 1	0.01269951	0.39605193
Q13508	ECTO-ADP-RIBOSYLTRANSFERASE 3	0.02551512	0.3757309
Q9Y646	CARBOXYPEPTIDASE Q	0.01082808	0.37419992
Q7Z7M9	POLYPEPTIDE N-ACETYLGALACTOSAMINYLTRANSFERASE 5	2.19E-05	0.35402838
Q13201	MULTIMERIN-1	0.01140993	0.34825216
P09486	SPARC	0.01052985	0.29001772
Q14980	NUCLEAR MITOTIC APPARATUS PROTEIN 1	0.01920018	0.28870117
Q9HCN6	PLATELET GLYCOPROTEIN VI	0.01447786	0.278601
P10319	HLA CLASS I HISTOCOMPATIBILITY ANTIGEN, B-58 ALPHA CHAIN	0.00313846	0.2524138
P02775	PLATELET BASIC PROTEIN	0.01501637	0.23579422
P19526	GALACTOSIDE 2-ALPHA-L-FUCOSYLTRANSFERASE 1	0.02776771	0.23568717
Q14766	LATENT-TRANSFORMING GROWTH FACTOR BETA-BINDING PROTEIN 1	0.03056464	0.2264809
P13647	KERATIN, TYPE II CYTOSKELETAL 5	0.0129735	0.18816533
P02751	FIBRONECTIN	0.0193273	0.16074162
P05067	AMYLOID BETA A4 PROTEIN	0.00255436	0.14595854
P40197	PLATELET GLYCOPROTEIN V	0.01181344	0.13467607
P07996	THROMBOSPONDIN-1	0.01814039	0.13158866
P35442	THROMBOSPONDIN-2	0.02800679	0.12677325

3.2.4 Functional annotation and enrichment of differential proteins between MI vs Sham groups

Up-regulated and down-regulated proteins underwent GO and KEGG functional analyses, respectively. According to GO functional annotation, proteins that were differentially expressed between the AD and Sham groups were mostly found in extracellular space and vesicles. It is involved in biological regulation, stimulation response, metabolic process, multicellular biological process, protein binding, ion binding, hydrolase activity and other biological functions (Fig.9, Fig.10). KEGG functional analysis revealed that the differentially expressed proteins between the MI and Sham groups were predominantly enriched in specific biological pathways (Fig. 11). These pathways included vesicle-mediated transport, immune response, cell secretion, cytoplasmic vesicle fraction, cell activation, proteolysis, secretory granules, exocytosis, regulated exocytosis, and leukocyte-mediated immunity. This clustering of differentially expressed proteins within these functionally related pathways suggests a coordinated alteration in cellular processes associated with MI pathogenesis. Notably, the enrichment of pathways related to exocytosis and vesicle transport indicates potential disruptions in cellular communication and signal transduction, which may contribute to the observed inflammatory response and tissue damage in MI. Further investigation into these pathways and their associated proteins could provide valuable insights into the molecular mechanisms underlying MI development and progression, thereby paving the way for the development of targeted therapeutic interventions.

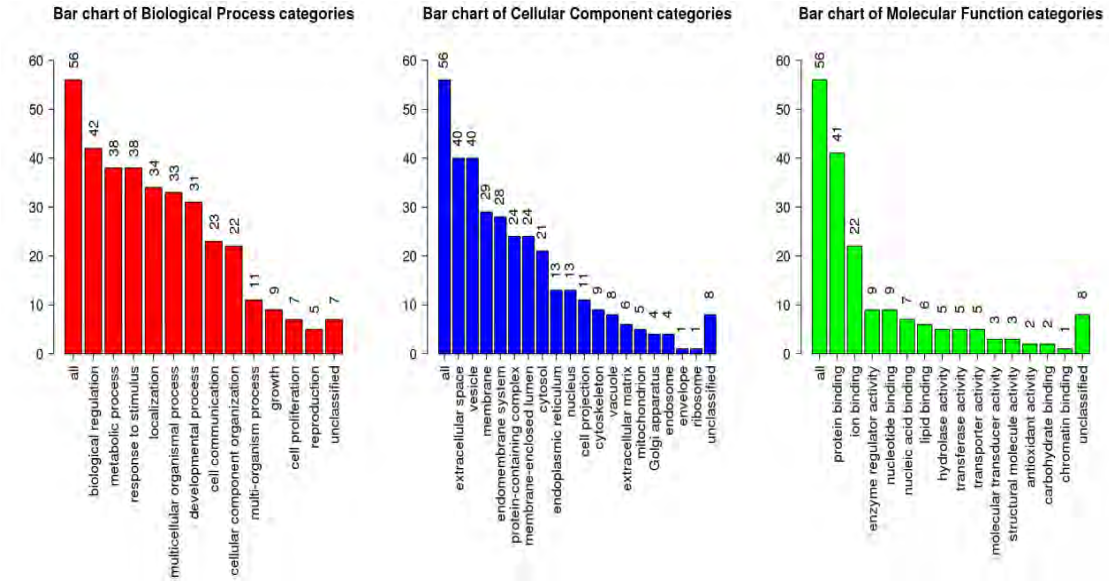

Figure 9: GO Slim overview of MI versus Sham up-regulated proteins. An individual red, blue, or green bar represents each biological Process, cellular component, and molecular function category. The number of IDs in the category and user lists is indicated by the height of the bar.

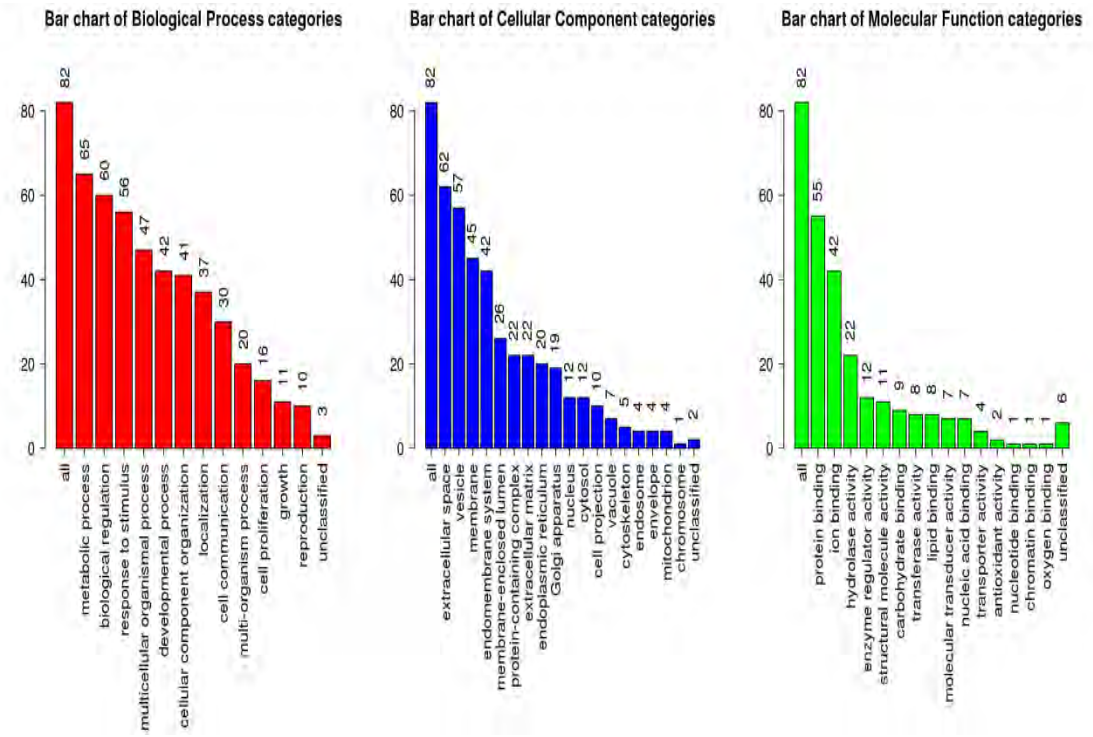

Figure 10: Summary of down-regulated proteins in MI as compared to Sham from GO Slim. An individual red, blue, or green bar represents each biological Process, cellular component, and molecular function category. The number of IDs in the category and user lists is indicated by the height of the bar.

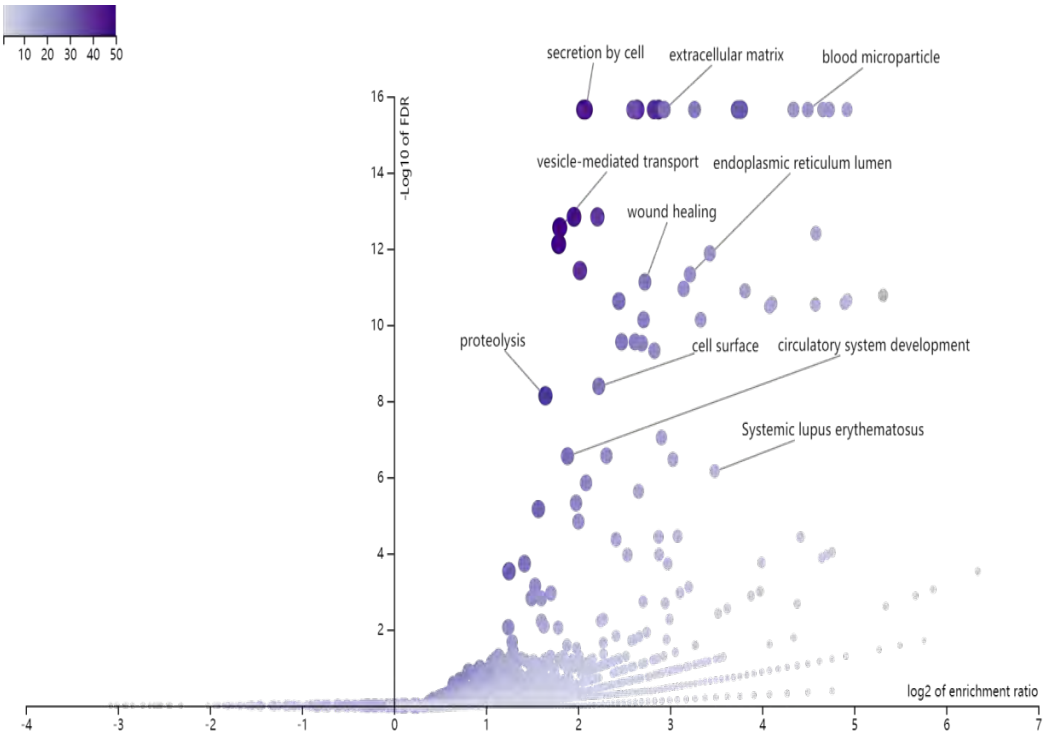

Figure 11: Volcano map shows the over-representation method's results for GO (GOBP, GOCC, and GOMF) and KEGG enrichment of up-regulated proteins in MI compared to Sham.

4. Comparison between ADvsSham groups

4.1 ADvsSham Principal component Analysis results

PCA analysis was performed on AD and Sham samples, and the results were shown in Fig.12. The two groups showed a certain classification trend in the PCA diagram, and the surface proteome changed between the two groups.

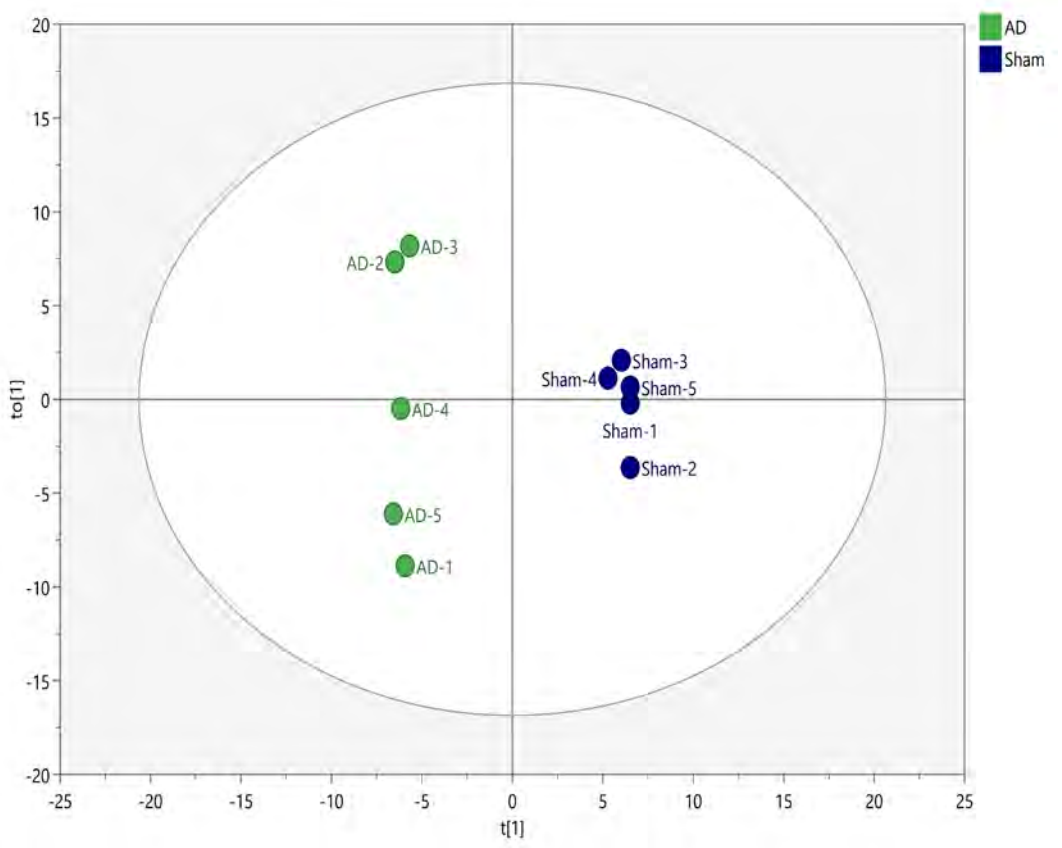

Figure 12: Metabolic phenotype unsupervised PCA score graphs comparing AD and Sham groups. For modeling, DIA proteomic data was log transformed and pareto scaled. Model specification: R2X=0.471 (cumulative variance proportion of 2 principal components).

4.2 Results of a discriminant analysis using orthogonal partial least squares between the AD and Sham groups

OPLS-DA classification results showed that the two groups of proteomic data were significantly different, Q2>0.5, the model had good predictive ability, and the model was effective (Fig. 13).

S-plot screened the metabolites with strong correlation of the main components (Fig. 14), and 100 times of displacement was used to test the robustness of OPLS-DA model. The intercepts of Q2 of the model was -0.153 and the slope was positive, indicating the robustness of the model (Fig. 15).

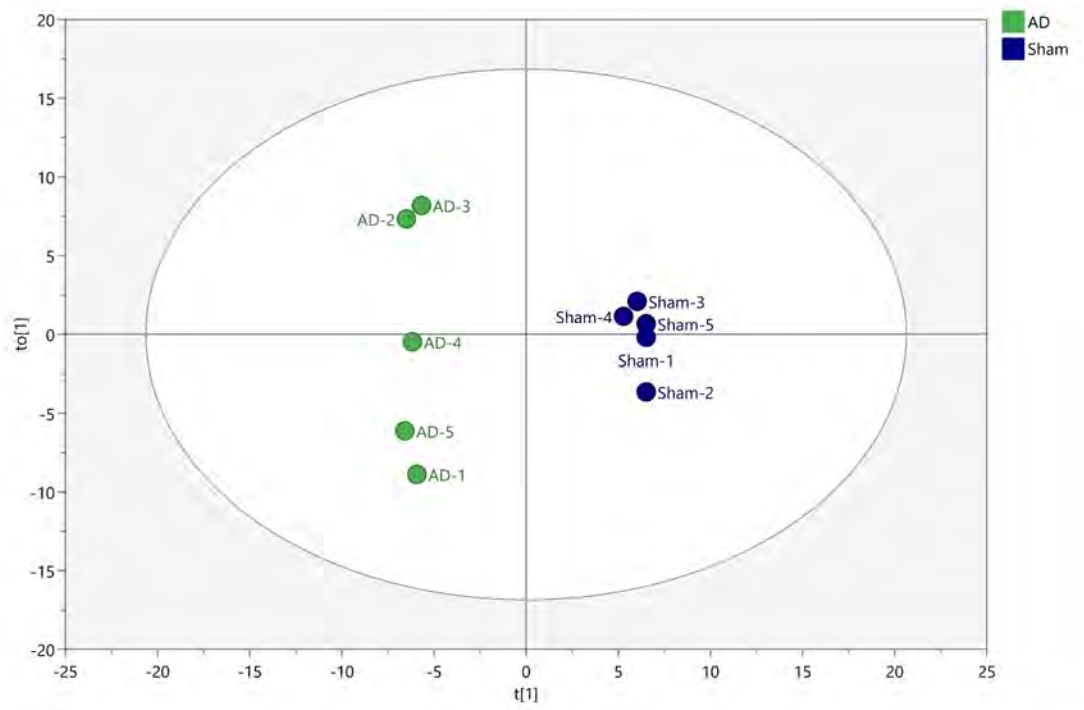

Figure 13: To maximize inter-group separation of metabolomic data between AD and Sham groups, OPLS-DA modeling score plot was used. Model specification: R2Y=0.996, Q2=0.849, 1 orthogonal + 1 predictive component.

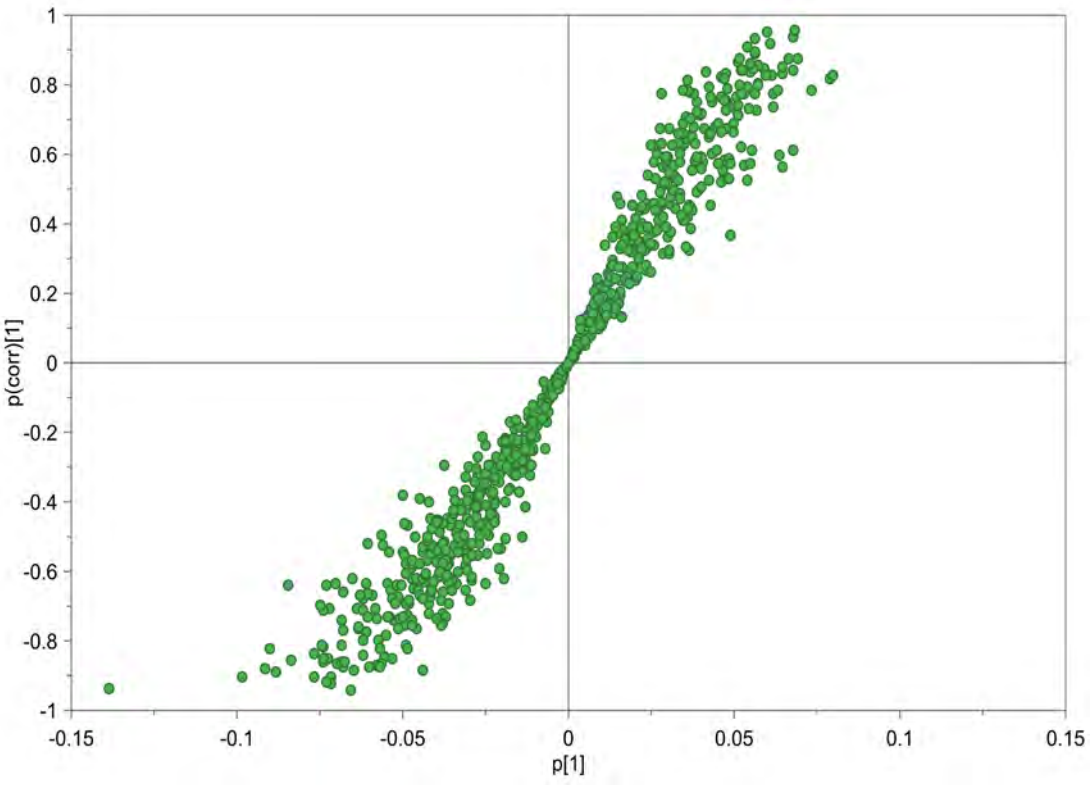

Figure 14: S-plot of OPLS-DA model between AD and Sham groups.

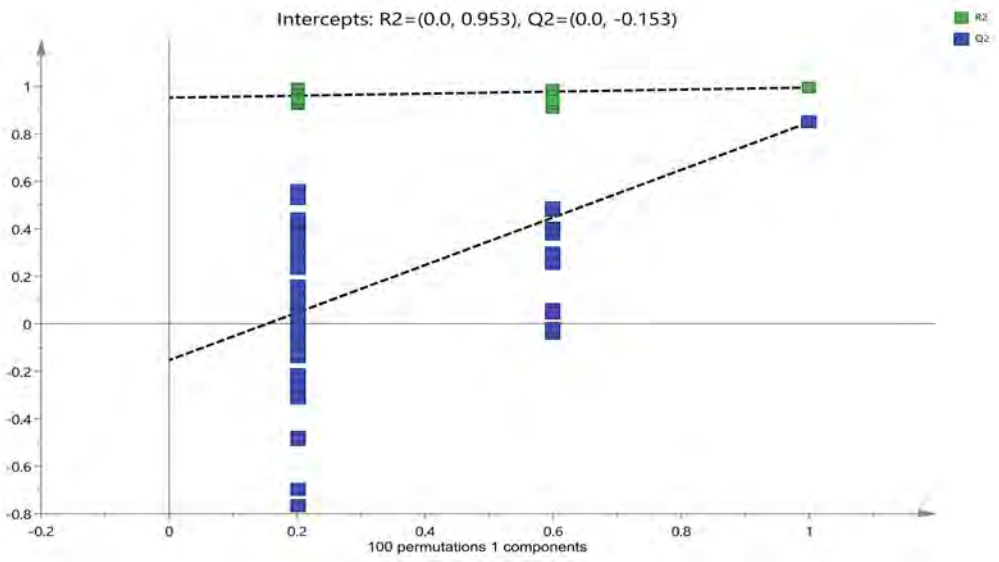

Figure 15: 100 times permutation to test robustness of OPLS-DA modeling.

4.3 Screening of differential proteins between AD and Sham groups

The quantitative protein data of the AD and Sham groups were subjected to a T-test, and the differentially expressed proteins between the two groups were screened with a P 0.05 cutoff. There were 195 proteins that were expressed differently, 101 of which were up-regulated (AD/Sham), and 94 of which were down-regulated (Fig. 16). Detailed differential protein information is shown in Tab. 3 and Tab.4.

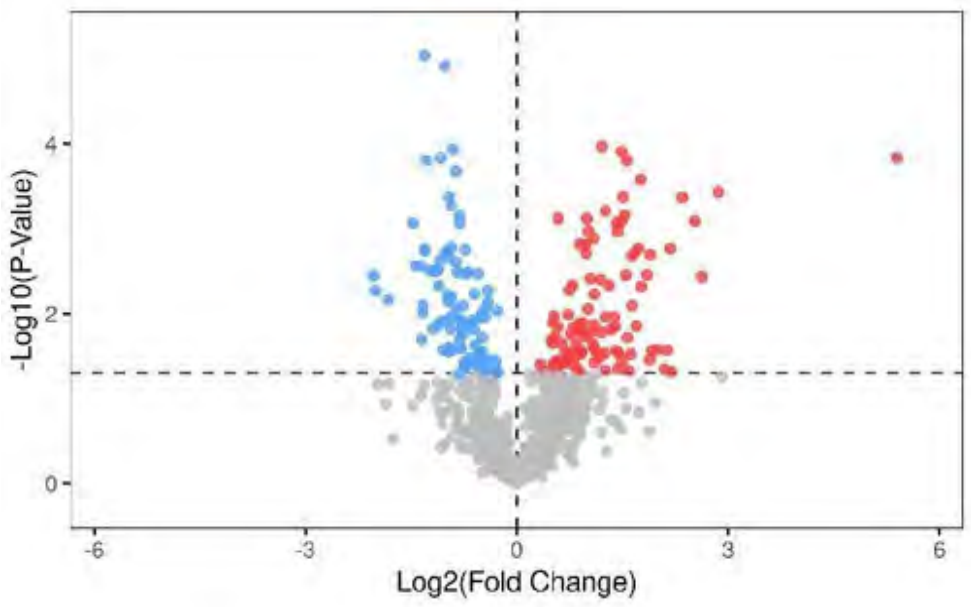

Figure 16 Visualizing AD and Sham using a volcano display utilizing quantitative DIA proteomics data. Proteins that had a significance level of p0.05 were highlighted in red. Each volcano plot showed the number of proteins that were up-regulated and those that were down-regulated.

Table 3(a) Up-expressed protein in AD in comparison to Sham (p<0.05)

UNIPROT ID	FIRST. PROTEIN. DESCRIPTION	P-VALUE	FOLD CHANGE
P0DJI8	SERUM AMYLOID A-1 PROTEIN	0.00014564	42.10673912
P02679	FIBRINOGEN GAMMA CHAIN	0.00037164	7.26563608
Q9Y279	V-SET AND IMMUNOGLOBULIN DOMAIN-CONTAINING PROTEIN 4	0.00369622	6.18614041
P02675	FIBRINOGEN BETA CHAIN	0.0008156	5.77113122
P36222	CHITINASE-3-LIKE PROTEIN 1	0.0004291	5.08869869
P35527	KERATIN, TYPE I CYTOSKELETAL 9	0.04830314	4.57362966
P01714	IG LAMBDA CHAIN V-III REGION SH	0.00170788	4.53087649
P01860	IG GAMMA-3 CHAIN C REGION	0.02681696	4.39632693
Q9BYE9	CADHERIN-RELATED FAMILY MEMBER 2	0.04479075	4.26616961
P08311	CATHEPSIN G	0.02646396	3.98676943
P24158	MYELOBLASTIN	0.0271376	3.77476741
P01861	IG GAMMA-4 CHAIN C REGION	0.00201734	3.71268917
P10645	CHROMOGRANIN-A	0.0346035	3.69481357
P80748	IG LAMBDA CHAIN V-III REGION LOI	0.00350799	3.59672905
P01717	IG LAMBDA CHAIN V-IV REGION HIL	0.0048114	3.40708088
P01609	IG KAPPA CHAIN V-I REGION SCW	0.00026259	3.38708389
P19652	ALPHA-1-ACID GLYCOPROTEIN 2	0.0017103	3.31084795
B9A064	IMMUNOGLOBULIN LAMBDA-LIKE POLYPEPTIDE 5	0.013979	3.24198801
P02763	ALPHA-1-ACID GLYCOPROTEIN 1	0.00191216	3.19494277
P35579	MYOSIN-9	0.00800927	3.1107617
P20827	EPHRIN-A1	0.00207973	3.10787596
P00738	HAPTOGLOBIN	0.03000329	3.06870147
P09211	GLUTATHIONE S-TRANSFERASE P	0.04673956	3.00157686
P08670	VIMENTIN	0.01902979	2.9681971
P07307	ASIALOGLYCOPROTEIN RECEPTOR 2	0.00015887	2.94416908
P18065	INSULIN-LIKE GROWTH FACTOR-BINDING PROTEIN 2	0.00352405	2.92583764
Q01518	ADENYLYL CYCLASE-ASSOCIATED PROTEIN 1	0.00069841	2.88790763
P30740	LEUKOCYTE ELASTASE INHIBITOR	0.000423	2.84997059
P52566	RHO GDP-DISSOCIATION INHIBITOR 2	0.03554796	2.82062932
P55287	CADHERIN-11	0.00012466	2.79830663
P01824	IG HEAVY CHAIN V-II REGION WAH	0.00081528	2.79823524
P04430	IG KAPPA CHAIN V-I REGION BAN	0.02908464	2.71318334
P05164	MYELOPEROXIDASE	0.04450835	2.70757794
P52209	6-PHOSPHOGLUCONATE DEHYDROGENASE, DECARBOXYLATING	0.001086	2.69448471

Table 3(b) Up-expressed protein in AD in comparison to Sham (p<0.05)

P04080	CYSTATIN-B	0.00084923	2.67850428
P05109	PROTEIN S100-A8	0.02724356	2.65417829
Q92496	COMPLEMENT FACTOR H-RELATED PROTEIN 4	0.01421381	2.62342636
P18428	LIPOPOLYSACCHARIDE-BINDING PROTEIN	0.01095168	2.61719962
P23083	IG HEAVY CHAIN V-I REGION V35	0.01525727	2.53791041
P78324	TYROSINE-PROTEIN PHOSPHATASE NON-RECEPTOR TYPE SUBSTRATE 1	0.00463858	2.47407955
P01833	POLYMERIC IMMUNOGLOBULIN RECEPTOR	0.00061808	2.3938363
P22455	FIBROBLAST GROWTH FACTOR RECEPTOR 4	0.01087454	2.38869611
Q15293	RETICULOCALBIN-1	0.04648657	2.38563882
P59666	NEUTROPHIL DEFENSIN 3	0.02928871	2.37537064
P13611	VERSICAN CORE PROTEIN	0.00010786	2.30798399
P09603	MACROPHAGE COLONY-STIMULATING FACTOR 1	0.01647096	2.3009408
P80188	NEUTROPHIL GELATINASE-ASSOCIATED LIPOCALIN	0.00398432	2.27623217
P15814	IMMUNOGLOBULIN LAMBDA-LIKE POLYPEPTIDE 1	0.0324739	2.25164771
P0CG05	IG LAMBDA-2 CHAIN C REGIONS	0.02826385	2.18488615
Q15063	PERIOSTIN	0.0376046	2.14531486
P0DMV8; P0DMV9	HEAT SHOCK 70 KDA PROTEIN 1A	0.00591923	2.14380406
P30044	PEROXIREDOXIN-5, MITOCHONDRIAL	0.01364786	2.13904905
P0C0L5	COMPLEMENT C4-B	0.02482979	2.13339656
P24821	TENASCIN	0.00130263	2.13300463
P10599	THIOREDOXIN	0.02264548	2.11561328
P01857	IG GAMMA-1 CHAIN C REGION	0.01607689	2.10855213
Q9HCB6	SPONDIN-1	0.003877	2.06427785
Q99536	SYNAPTIC VESICLE MEMBRANE PROTEIN VAT-1 HOMOLOG	0.00106501	2.0247618
Q02487	DESMOCOLLIN-2	0.00878106	2.01520757
P22692	INSULIN-LIKE GROWTH FACTOR-BINDING PROTEIN 4	0.0007606	1.9956667
P02452	COLLAGEN ALPHA-1(I) CHAIN	0.01845146	1.98182366
P37837	TRANSALDOLASE	0.00194166	1.98177761
Q12866	TYROSINE-PROTEIN KINASE MER	0.00154456	1.96522485
P01009	ALPHA-1-ANTITRYPSIN	0.01660229	1.92427073

Table 3(c) Up-expressed protein in AD in comparison to Sham (p<0.05)

P19320	VASCULAR CELL ADHESION PROTEIN 1	0.01278921	1.90639485
Q02985	COMPLEMENT FACTOR H-RELATED PROTEIN 3	0.02816268	1.89679939
P02750	LEUCINE-RICH ALPHA-2-GLYCOPROTEIN	0.02960391	1.88463125
Q92736	RYANODINE RECEPTOR 2	0.012998	1.86821084
P07711	CATHEPSIN L1	0.02737862	1.85349653
P01034	CYSTATIN-C	0.00152153	1.8528883
P31146	CORONIN-1A	0.04636303	1.8468527
P09960	LEUKOTRIENE A-4 HYDROLASE	0.01572812	1.8101572
P26358	DNA (CYTOSINE-5)-METHYLTRANSFERASE 1	0.02241635	1.80116562
P02656	APOLIPOPROTEIN C-III	0.04263203	1.78249475
P07900	HEAT SHOCK PROTEIN HSP 90-ALPHA	0.032873	1.76181861
P01598	IG KAPPA CHAIN V-I REGION EU	0.01450838	1.74801907
P28799	GRANULINS	0.00462233	1.72637347
P41222	PROSTAGLANDIN-H2 D-ISOMERASE	0.02909849	1.70097952
P02748	COMPLEMENT COMPONENT C9	0.01753822	1.69895851
P01011	ALPHA-1-ANTICHYMOTRYPSIN	0.00530909	1.67420358
P01611	IG KAPPA CHAIN V-I REGION WES	0.01035423	1.65615586
P07858	CATHEPSIN B	0.03333559	1.65019761
P10586	RECEPTOR-TYPE TYROSINE-PROTEIN PHOSPHATASE F	0.03791294	1.6248628
P08123	COLLAGEN ALPHA-2(I) CHAIN	0.02721425	1.61546492
O00468	AGRIN	0.03641814	1.59476961
Q9UBX5	FIBULIN-5	0.02257799	1.56049655
P06703	PROTEIN S100-A6	0.0425731	1.50106899
P61626	LYSOZYME C	0.00075836	1.49964743
P06733	ALPHA-ENOLASE	0.03762138	1.49843104
Q9Y4L1	HYPOXIA UP-REGULATED PROTEIN 1	0.01421326	1.49779941
P80723	BRAIN ACID SOLUBLE PROTEIN 1	0.03530762	1.48728483
Q14118	DYSTROGLYCAN	0.04563157	1.48406955
P02671	FIBRINOGEN ALPHA CHAIN	0.01846239	1.45687623
Q86U17	SERPIN A11	0.01064079	1.44099531
P01008	ANTITHROMBIN-III	0.03848034	1.43278956
P15151	POLIOVIRUS RECEPTOR	0.0223923	1.42560211
Q15828	CYSTATIN-M	0.01280204	1.4223026
P39060	COLLAGEN ALPHA-1(XVIII) CHAIN	0.02033893	1.40214593
P15907	BETA-GALACTOSIDE ALPHA-2,6-SIALYLTRANSFERASE 1	0.04663953	1.39223693
P24387	CORTICOTROPIN-RELEASING FACTOR-BINDING PROTEIN	0.04858997	1.30771282
Q9BXR6	COMPLEMENT FACTOR H-RELATED PROTEIN 5	0.03953042	1.25966912

Table 4(a) Down-expressed protein in AD in comparison to Sham (p<0.05)

UNIPROT ID	FIRST.PROTEIN. DESCRIPTION	P-VALUE	FOLD CHANGE
P04180	Phosphatidylcholine-sterol acyltransferase	0.04918615	0.83172017
Q96IY4	Carboxypeptidase B2	0.00930496	0.82600873
P01042	Kininogen-1	0.04845841	0.82001315
P19823	Inter-alpha-trypsin inhibitor heavy chain H2	0.03716539	0.81484727
P22792	Carboxypeptidase N subunit 2	0.04168674	0.79141196
O00533	Neural cell adhesion molecule L1-like protein	0.03548894	0.78191609
P98160	Basement membrane-specific heparan sulfate proteoglycan core protein	0.00721193	0.75330796
Q04756	Hepatocyte growth factor activator	0.0053557	0.749999
Q99784	Noelin	0.04650331	0.74264907
Q76LX8	A disintegrin and metalloproteinase with thrombospondin motifs 13	0.04517454	0.74132364
P48740	Mannan-binding lectin serine protease 1	0.0085319	0.73864029
P43121	Cell surface glycoprotein MUC18	0.03452557	0.73497012
P30101	Protein disulfide-isomerase A3	0.01105687	0.73343909
P00747	Plasminogen	0.03556766	0.72437782
P10124	Serglycin	0.04243174	0.71797024
P08195	4F2 cell-surface antigen heavy chain	0.00981551	0.71365464
P11279	Lysosome-associated membrane glycoprotein 1	0.01913442	0.71324048
Q13822	Ectonucleotide pyrophosphatase/phosphodiesterase family member 2	0.02912739	0.70908453
P20851	C4b-binding protein beta chain	0.02818883	0.70659242
Q9Y6Z7	Collectin-10	0.02729213	0.69297082
P49641	Alpha-mannosidase 2x	0.01143655	0.68988495
Q12913	Receptor-type tyrosine-protein phosphatase eta	0.00338829	0.6841884
Q08380	Galectin-3-binding protein	0.03451896	0.68074341
P05543	Thyroxine-binding globulin	0.03530873	0.67402562
P43251	Biotinidase	0.04004755	0.66946344
P16035	Metalloproteinase inhibitor 2	0.023494	0.66167388
P05546	Heparin cofactor 2	0.00587159	0.65890277
P09486	SPARC	0.01547933	0.65608397
Q6YHK3	CD109 antigen	0.01183748	0.64853543
P08185	Corticosteroid-binding globulin	0.03287646	0.63119547
Q9H4A3	Serine/threonine-protein kinase WNK1	0.01365199	0.63057361
O75882	Attractin	0.00325175	0.61850521
P51884	Lumican	0.01325443	0.60858987
Q01459	Di-N-acetylchitobiase	0.03980143	0.60396342
P07225	Vitamin K-dependent protein S	0.0017644	0.60112855
Q96RD9	Fc receptor-like protein 5	0.00338238	0.60034142

Table 4(b) Down-expressed protein in AD in comparison to Sham (p<0.05)

Q9UNN8	Endothelial protein C receptor	0.04058233	0.59956967
P04066	Tissue alpha-L-fucosidase	0.041528	0.59845471
P06727	Apolipoprotein A-IV	0.03732076	0.59597793
Q12860	Contactin-1	0.01712087	0.59039849
P02751	Fibronectin	0.00810447	0.58672201
Q7Z7M0	Multiple epidermal growth factor-like domains protein 8	0.01223779	0.58330429
P23142	Fibulin-1	0.01494538	0.58165438
Q15067	Peroxisomal acyl-coenzyme A oxidase 1	0.02548766	0.57898789
Q5VU43	Myomegalin	0.0251955	0.57350106
Q9Y646	Carboxypeptidase Q	0.04992402	0.57219684
P43652	Afamin	0.01983485	0.56919256
P13591	Neural cell adhesion molecule 1	0.00087038	0.56894916
P27169	Serum paraoxonase/arylesterase 1	0.00069638	0.56769531
P02652	Apolipoprotein A-II	0.01156586	0.56496525
P55290	Cadherin-13	0.00326801	0.55734473
Q16853	Membrane primary amine oxidase	0.00836924	0.55240639
P00734	Prothrombin	0.00021114	0.54993852
Q9UHG3	Prenylcysteine oxidase 1	0.00247222	0.54910243
P08709	Coagulation factor VII	0.00011598	0.53616205
Q92835	Phosphatidylinositol 3,4,5-trisphosphate 5-phosphatase 1	0.02684575	0.53398319
P35443	Thrombospondin-4	0.01056763	0.52934836
P49747	Cartilage oligomeric matrix protein	0.00167101	0.52748027
O75636	Ficolin-3	0.00629429	0.5234986
Q9UBQ6	Exostosin-like 2	0.00053333	0.52208708
P00748	Coagulation factor XII	0.01511904	0.52120052
P06396	Gelsolin	0.00215826	0.5145975
P00742	Coagulation factor X	0.00042278	0.51423241
P04745	Alpha-amylase 1	0.02816526	0.51211523
P78552	Interleukin-13 receptor subunit alpha-1	0.0246986	0.51196748
P10619	Lysosomal protective protein	0.00715218	0.50710555
P05556	Integrin beta-1	0.00599821	0.50485965
Q5CZC0	Fibrous sheath-interacting protein 2	0.01183314	0.50341272
P12955	Xaa-Pro dipeptidase	0.00181131	0.50270014
P05452	Tetranectin	0.00190825	0.49727281
P04070	Vitamin K-dependent protein C	1.21E-05	0.49375506
P13497	Bone morphogenetic protein 1	0.02684845	0.48391943
Q8IUK5	Plexin domain-containing protein 1	0.01228227	0.47684015
P40197	Platelet glycoprotein V	0.00014595	0.47341174
P04196	Histidine-rich glycoprotein	0.00231441	0.47107065
P54108	Cysteine-rich secretory protein 3	0.00470835	0.46307189

Table 4(c) Down-expressed protein in AD in comparison to Sham (p<0.05)

P06276	Cholinesterase	0.01369771	0.46261003
P22105	Tenascin-X	0.00298141	0.45985826
P07996	Thrombospondin-1	0.0031907	0.45117163
P27824	Calnexin	0.0150602	0.43782905
P28906	Hematopoietic progenitor cell antigen CD34	0.00313618	0.42770436
P10721	Mast/stem cell growth factor receptor Kit	0.00015857	0.4117417
Q9NQ79	Cartilage acidic protein 1	0.00182684	0.40376165
Q8IUL8	Cartilage intermediate layer protein 2	0.00174652	0.40305295
Q96KN2	Beta-Ala-His dipeptidase	9.21E-06	0.40285258
P54289	Voltage-dependent calcium channel subunit alpha-2/delta-1	0.00792834	0.39685411
Q6UXB8	Peptidase inhibitor 16	0.0096332	0.3957569
Q12884	Prolyl endopeptidase FAP	0.01992852	0.39245648
Q9BXJ4	Complement C1q tumor necrosis factor-related protein 3	0.00273632	0.3902246
P07911	Uromodulin	0.0027388	0.36876621
P35442	Thrombospondin-2	0.00086041	0.35916964
P05106	Integrin beta-3	0.00686771	0.28127721
P23141	Liver carboxylesterase 1	0.00534592	0.24970847
P22891	Vitamin K-dependent protein Z	0.00358366	0.24376863

4.4 Functional annotation and enrichment of differential proteins between AD and Sham groups

Up-regulated and down-regulated proteins underwent GO and KEGG functional analyses, respectively. According to GO functional annotation, proteins that were differentially expressed between the AD and Sham groups were mostly found in extracellular space and vesicles.

It is involved in biological regulation, stimulation response, metabolic processes, processes of multicellular organisms, protein binding, ion binding, hydrolase activity and other biological functions (Fig.17, Fig.18). Through cells, cell activation, immune effector mechanisms, leukocyte-mediated immunity, endoplasmic reticulum, cell movement, collagen-containing extracellular matrix, extracellular matrix, wound healing, secretion granules, and exocytosis regulation, KEGG functional analysis revealed that differential proteins between AD and Sham groups were primarily enriched in cytoplasmic vesicles (Fig.19).

Furthermore, these vesicles are crucial for the transport and communication of signaling molecules within the cell, playing a vital role in cellular homeostasis and development. Additionally, they contribute to the process of endocytosis, essential for the uptake of nutrients and other molecules into the cell. Understanding the role of these vesicles in healthy and

diseased states could provide valuable insights for the development of novel therapeutic interventions.

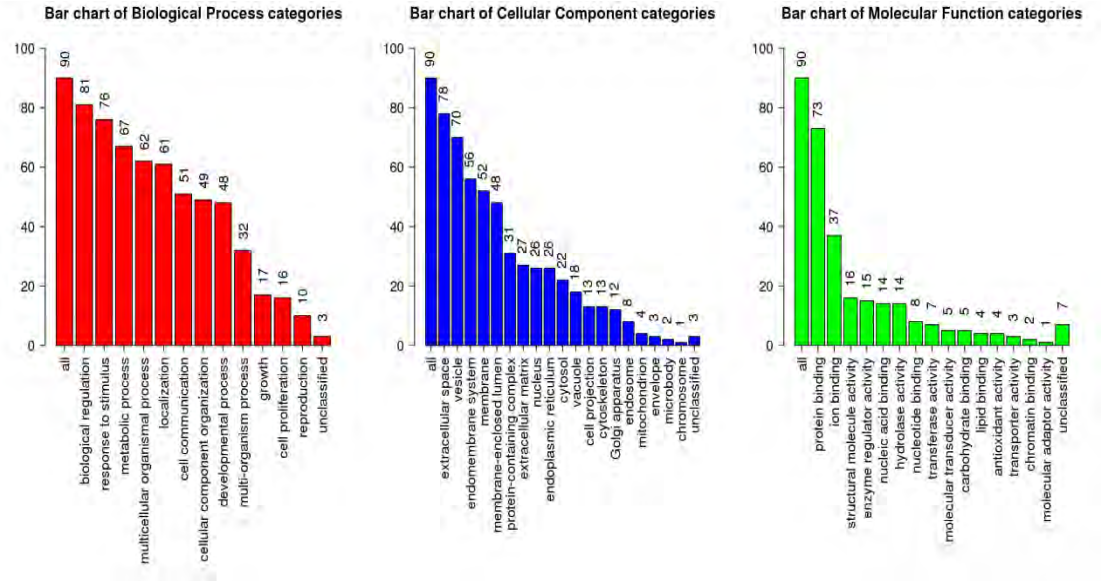

Figure 17: Proteins that are upregulated in AD relative to Sham are summarized by GO Slim. An individual red, blue, or green bar represents each biological Process, cellular component, and molecular function category. The number of IDs in the category and user lists is indicated by the height of the bar.

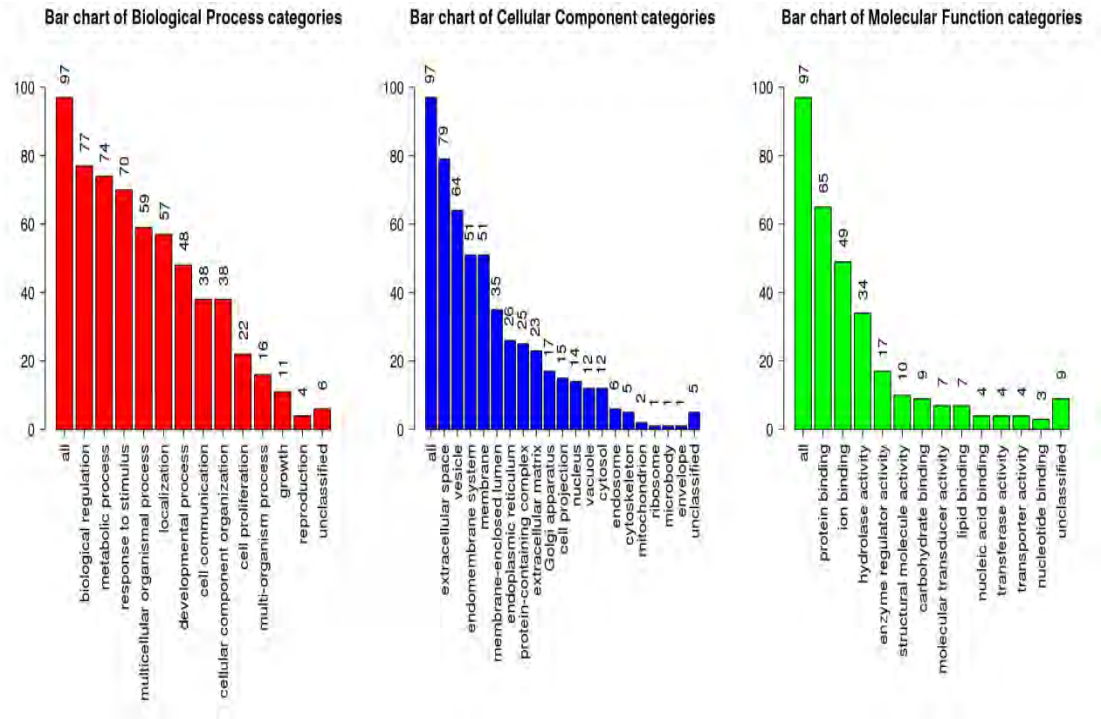

Figure 18: Summary of proteins that are down-regulated in AD compared to Sham using GO Slim. An individual red, blue, or green bar represents each biological Process, cellular component, and molecular function category. The number of IDs in the category and user lists is indicated by the height of the bar.

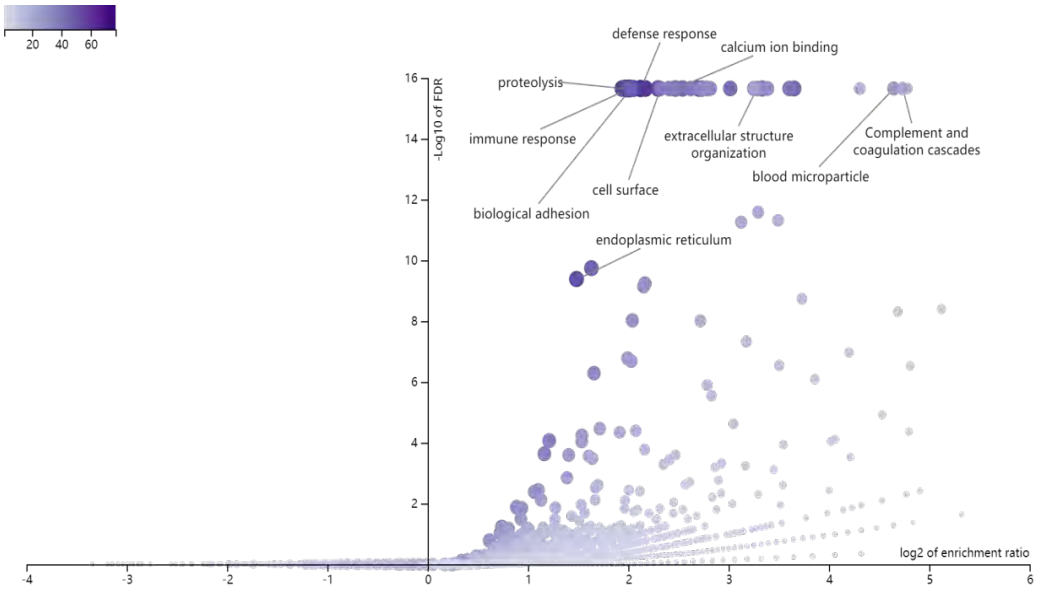

Figure 19: Employing the over representation method, a volcano plot of GO (GOBP, GOCC, and GOMF) and KEGG enrichment results of up-regulated proteins in AD compared to Sham was created.

4.5 Comparison between AD and MI groups

4.5.1 AD vs MI principal component analysis results

PCA analysis was performed on AD and MI samples, and the results were shown in Fig. 20. The two groups showed a certain classification trend in the PCA diagram, and the surface proteome changed between the two groups.

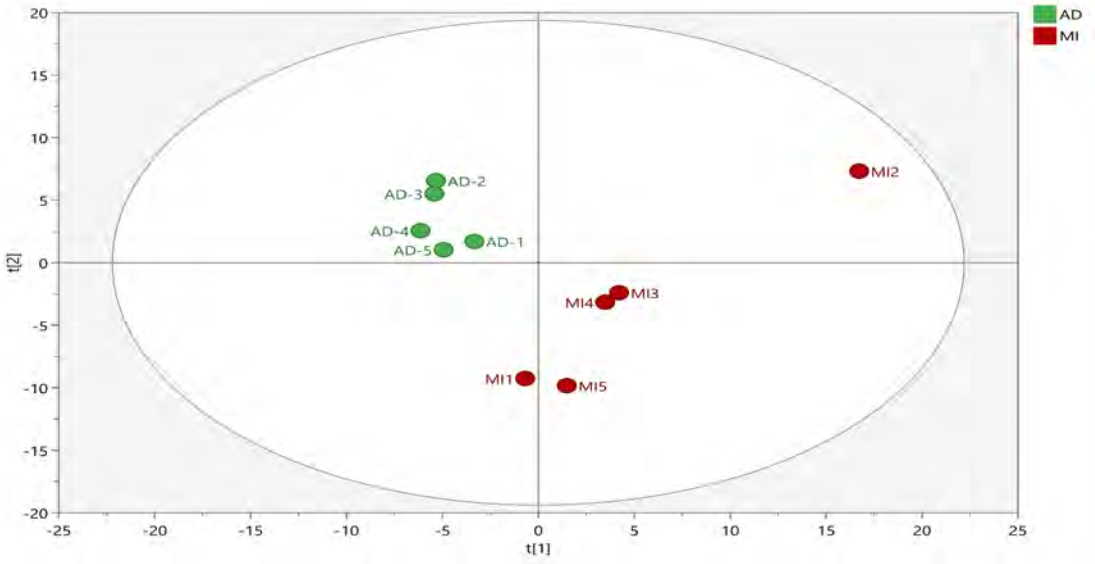

Figure 20: Unsupervised PCA score plots of metabolic phenotypes between AD and MI groups. Model parameter: R2X=0.471

4.5.2 Results of a discriminant analysis using orthogonal partial least square

The proteomic data of the two groups were significantly different, with Q2>0.5, and the model had good predictive ability and was effective (Fig. 21). S-plot screened the metabolites with strong correlation of the main components (Fig. 22). The robustness of OPLS-DA model was tested by 100 permutation tests, and the intercepts of Q2 of the model prediction ability was -0.183 and the slope was positive, indicating the robustness of the model (Fig. 23).

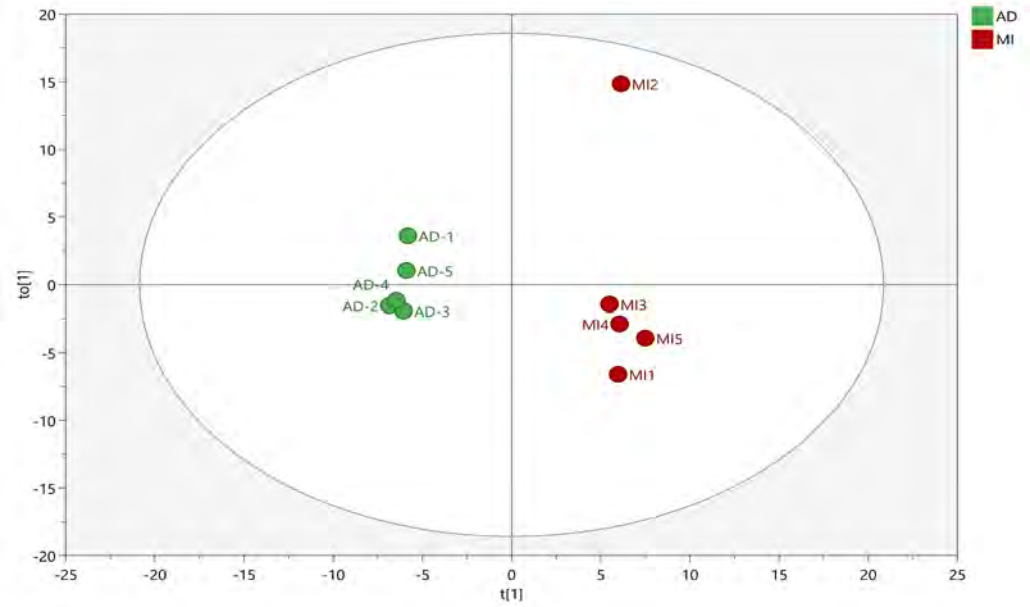

Figure 21: To maximize inter-group separation of metabolomic data between AD and MI groups, OPLS-DA modeling score plot was used. Model parameters: R2Y=0.992, Q2=0.812, 1 orthogonal and 1 predictive component.

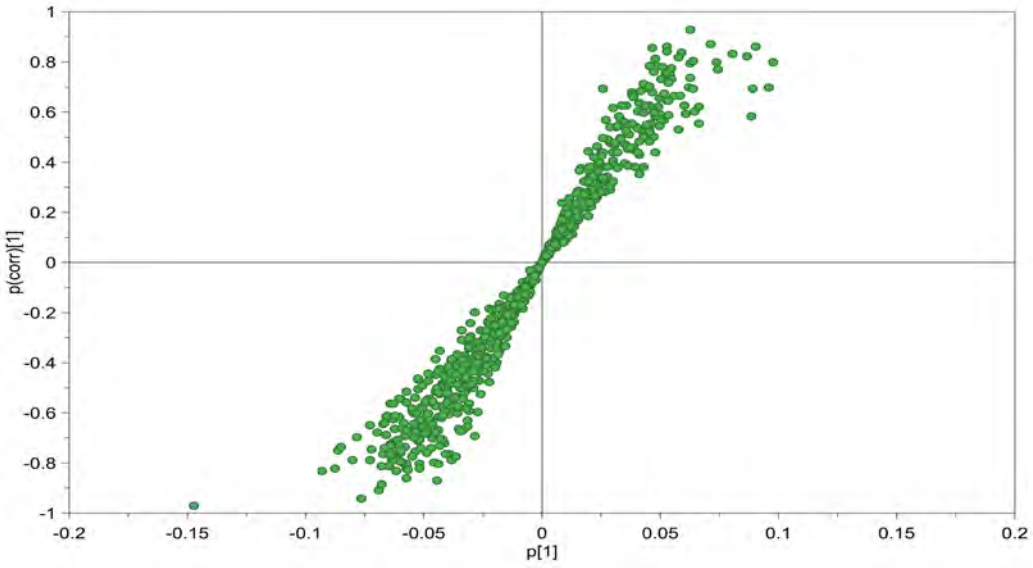

Figure 22: S-plot of OPLS-DA model between **AD and MI** groups.

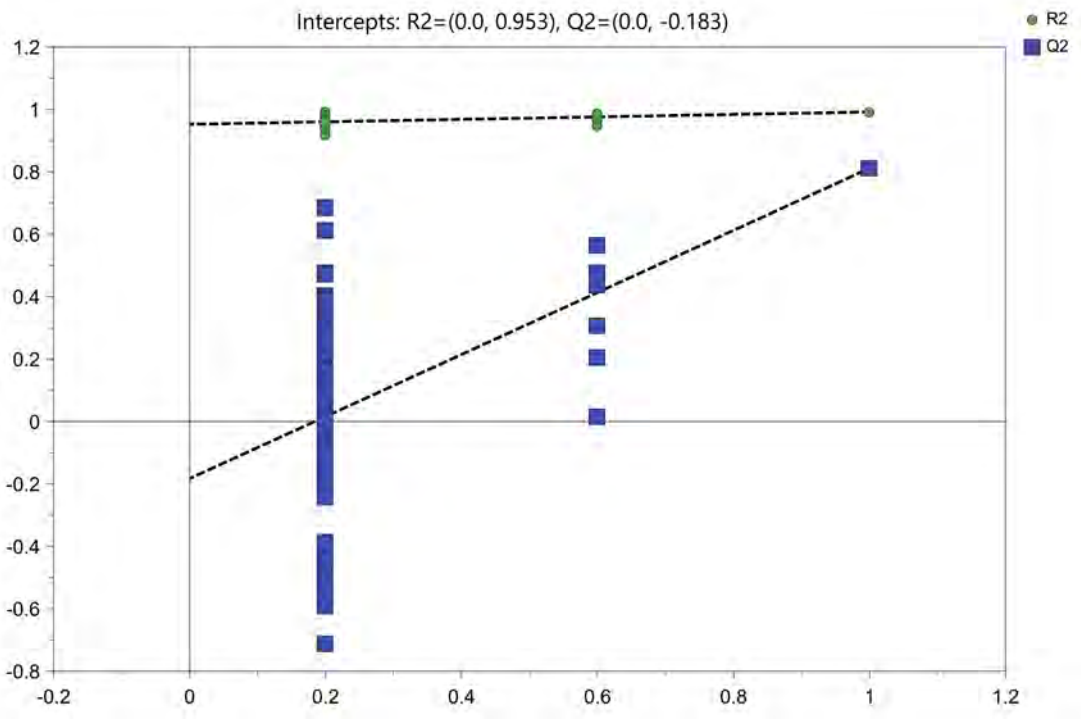

Figure 23: 100 times permutation to test robustness of OPLS-DA modeling.

4.5.3 Differential proteins between AD and MI groups

T-test was performed on the quantitative protein results of the AD and MI groups, and the differentially expressed proteins between the two groups were screened with P <0.05 as the threshold. A total of 143 proteins showed differentially expressed, with 93 proteins were up-regulated (AD/MI) and 50 proteins were down-regulated (Fig. 24). Detailed differential protein information is shown in Tab.5 and Tab. 6.

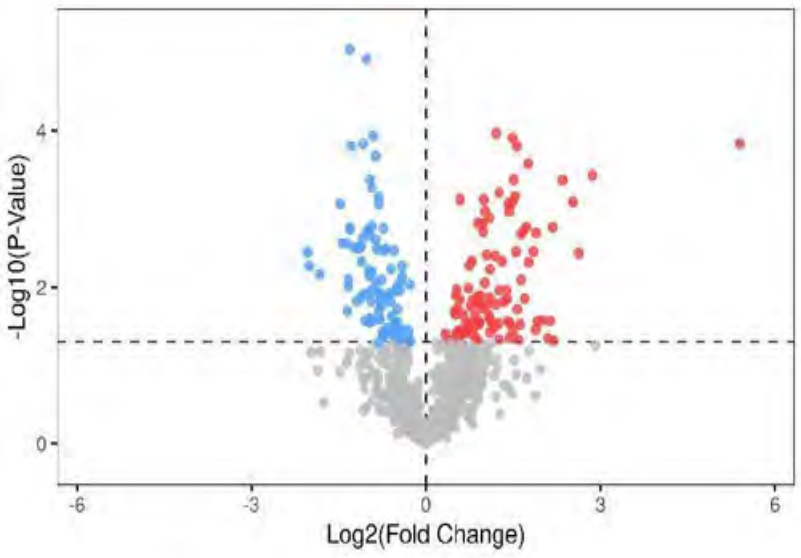

Figure 24: Volcanic map, p<0.05 for significantly expressed proteins are highlighted in red.

Table 5(a) Up-expressed protein in AD in comparison to MI (p<0.05)

UNIPROT ID	FIRST. PROTEIN. DESCRIPTION	P-VALUE	FOLD CHANGE
P0DJI8	SERUM AMYLOID A-1 PROTEIN	4.83E-06	67.60713333
P19652	ALPHA-1-ACID GLYCOPROTEIN 2	0.00243227	7.45984311
P18428	LIPOPOLYSACCHARIDE-BINDING PROTEIN	0.01411945	6.41496201
P13647	KERATIN, TYPE II CYTOSKELETAL 5	0.01785702	6.0790705
P0C0L5	COMPLEMENT C4-B	0.02004096	5.51233771
P05067	AMYLOID BETA A4 PROTEIN	0.00638272	5.45405089
P19526	GALACTOSIDE 2-ALPHA-L-FUCOSYLTRANSFERASE 1	0.03940034	4.77956396
Q9HCN6	PLATELET GLYCOPROTEIN VI	0.0098526	4.54161648
P08311	CATHEPSIN G	0.04487708	3.82212702
P02763	ALPHA-1-ACID GLYCOPROTEIN 1	0.01549394	3.69071951
P10319	HLA CLASS I HISTOCOMPATIBILITY ANTIGEN, B-58 ALPHA CHAIN	0.00775667	3.48374701
P07307	ASIALOGLYCOPROTEIN RECEPTOR 2	3.39E-05	3.25507339
P04259	KERATIN, TYPE II CYTOSKELETAL 6B	0.04754474	3.18288468
P02775	PLATELET BASIC PROTEIN	0.03803529	3.11578988
P80188	NEUTROPHIL GELATINASE-ASSOCIATED LIPOCALIN	0.01044495	3.06939258
Q13508	ECTO-ADP-RIBOSYLTRANSFERASE 3	0.01816	3.04237127
O76076	WNT1-INDUCIBLE-SIGNALING PATHWAY PROTEIN 2	0.03972931	2.99148337
Q15828	CYSTATIN-M	0.00412558	2.92895418
P41222	PROSTAGLANDIN-H2 D-ISOMERASE	0.01831555	2.90002633
P02786	TRANSFERRIN RECEPTOR PROTEIN 1	0.02801462	2.85081954
P05164	MYELOPEROXIDASE	0.04059519	2.83352192
Q9HDC9	ADIPOCYTE PLASMA MEMBRANE-ASSOCIATED PROTEIN	0.00764933	2.80841389
Q7Z7M9	POLYPEPTIDE N-ACETYLGALACTOSAMINYLTRANSFERASE 5	0.00010669	2.7528373
P18065	INSULIN-LIKE GROWTH FACTOR-BINDING PROTEIN 2	0.02079833	2.73257787
Q15063	PERIOSTIN	0.01464281	2.72149533
P09603	MACROPHAGE COLONY-STIMULATING FACTOR 1	0.02156692	2.70582538

Table 5(b) Up-expressed protein in AD in comparison to MI (p<0.05)

Q13201	MULTIMERIN-1	0.02788921	2.69705693
P14780	MATRIX METALLOPROTEINASE-9	0.03107936	2.67946633
P06702	PROTEIN S100-A9	0.04908024	2.67165273
P24821	TENASCIN	0.00118258	2.63838254
P01009	ALPHA-1-ANTITRYPSIN	0.00562207	2.62633137
Q9Y240	C-TYPE LECTIN DOMAIN FAMILY 11 MEMBER A	0.02138257	2.61904035
P34096	RIBONUCLEASE 4	0.0054412	2.58602064
P05109	PROTEIN S100-A8	0.02085632	2.58425158
O75594	PEPTIDOGLYCAN RECOGNITION PROTEIN 1	0.00837431	2.58248414
P07602	PROSAPOSIN	0.02903753	2.56751639
Q14118	DYSTROGLYCAN	0.01732392	2.54025885
Q86UD1	Out at first protein homolog	0.04051575	2.48255715
Q96S96	Phosphatidylethanolamine-binding protein 4	0.01296798	2.46083359
P55287	Cadherin-11	0.01303418	2.41710671
P01033	Metalloproteinase inhibitor 1	0.01407965	2.36261186
P52209	6-phosphogluconate dehydrogenase, decarboxylating	0.03284245	2.36095453
P01034	Cystatin-C	0.00387056	2.35586079
Q06033	Inter-alpha-trypsin inhibitor heavy chain H3	0.01977779	2.33684058
P0C0L4	Complement C4-A	0.02338072	2.31265332
Q86U17	Serpin A11	0.00893083	2.3061752
P21709	Ephrin type-A receptor 1	0.04891946	2.28602031
P61626	Lysozyme C	0.00658499	2.27402935
P22455	Fibroblast growth factor receptor 4	0.04386916	2.26528367
Q9Y4L1	Hypoxia up-regulated protein 1	0.02433216	2.24561142
Q9Y274	Type 2 lactosamine alpha-2,3-sialyltransferase	0.04656843	2.20762469
P27797	Calreticulin	0.00512149	2.16532011
P02750	Leucine-rich alpha-2-glycoprotein	0.00481231	2.14989117
P35542	Serum amyloid A-4 protein	0.0383008	2.13020147
P24592	Insulin-like growth factor-binding protein 6	0.00416621	2.10450588
Q16706	Alpha-mannosidase 2	0.0035699	2.07367184
P02748	Complement component C9	0.00849398	2.07317023
P26358	DNA (cytosine-5)-methyltransferase 1	0.03322148	2.04800412
Q12866	Tyrosine-protein kinase Mer	0.02381933	2.04200166
P22692	Insulin-like growth factor-binding protein 4	0.00142345	2.04183415
P02452	Collagen alpha-1(I) chain	0.04070171	2.02181462
P08123	Collagen alpha-2(I) chain	0.01584963	2.01515535

Table 5(c) Up-expressed protein in AD in comparison to MI ($p<0.05$)

P13598	Intercellular adhesion molecule 2	0.02788378	2.01508006
P01772	Ig heavy chain V-III region KOL	0.04895538	1.99738594
P19320	Vascular cell adhesion protein 1	0.03977926	1.97755205
P61769	Beta-2-microglobulin	0.02972128	1.97407456
P78324	Tyrosine-protein phosphatase non-receptor type substrate 1	0.02919057	1.94714666
P19021	Peptidyl-glycine alpha-amidating monooxygenase	0.00402088	1.91145727
P24593	Insulin-like growth factor-binding protein 5	0.04212879	1.88205684
P14543	Nidogen-1	0.02443412	1.88078605
O43505	Beta-1,4-glucuronyltransferase 1	0.00323722	1.86477624
Q86SQ4	G-protein coupled receptor 126	0.01017632	1.81225104
Q9NZ08	Endoplasmic reticulum aminopeptidase 1	0.04994263	1.79352344
P36955	Pigment epithelium-derived factor	0.03002364	1.78028218
O95479	GDH/6PGL endoplasmic bifunctional protein	0.03044306	1.74629837
P59666	Neutrophil defensin 3	0.01649303	1.73494251
Q02487	Desmocollin-2	0.04087815	1.68299389
P15151	Poliovirus receptor	0.02069621	1.6697296
P09871	Complement C1s subcomponent	0.01452417	1.63345604
P07359	Platelet glycoprotein Ib alpha chain	0.00814302	1.61182017
P00751	Complement factor B	0.01367913	1.59035188
Q10471	Polypeptide N-acetylgalactosaminyltransferase 2	0.00454486	1.58218193
P13796	Plastin-2	0.03613506	1.54801647
P13671	Complement component C6	0.00095814	1.54681383
Q6EMK4	Vasorin	0.01307725	1.4933459
P10909	Clusterin	0.00792031	1.46974639
P05156	Complement factor I	0.00548429	1.42964027
P01591	Immunoglobulin J chain	0.03865239	1.42265054
Q76LX8	A disintegrin and metalloproteinase with thrombospondin motifs 13	0.02390711	1.41947564
Q14624	Inter-alpha-trypsin inhibitor heavy chain H4	0.01165423	1.38055902
P15144	Aminopeptidase N	0.04862681	1.35270569
P24387	Corticotropin-releasing factor-binding protein	0.03609313	1.23580693

Table 6(a) Down-expressed protein in AD in comparison to MI (p<0.05)

UNIPROT ID	FIRST.PROTEIN. DESCRIPTION	P-VALUE	FOLD CHANGE
Q04756	Hepatocyte growth factor activator	0.02561035	0.83378216
Q15262	Receptor-type tyrosine-protein phosphatase kappa	0.04561233	0.67854428
P46531	Neurogenic locus notch homolog protein 1	0.04876835	0.67604687
P51884	Lumican	0.03317899	0.65765041
Q12860	Contactin-1	0.02797521	0.64028752
P14618	Pyruvate kinase PKM	0.02674138	0.63819166
Q96KN2	Beta-Ala-His dipeptidase	0.00315065	0.62817315
P05452	Tetranectin	0.00794308	0.61222403
Q08380	Galectin-3-binding protein	0.02626665	0.60938707
P28906	Hematopoietic progenitor cell antigen CD34	0.04884018	0.60655475
P07225	Vitamin K-dependent protein S	0.02996526	0.60638934
P43121	Cell surface glycoprotein MUC18	0.01455829	0.59998515
Q9ULI3	Protein HEG homolog 1	0.02910605	0.57938341
Q16853	Membrane primary amine oxidase	0.00276378	0.5740873
P02787	Serotransferrin	0.01078767	0.57289021
P04070	Vitamin K-dependent protein C	0.00583092	0.56451426
P08294	Extracellular superoxide dismutase [Cu-Zn]	0.04394645	0.55635311
P08709	Coagulation factor VII	0.0009673	0.53750158
P02792	Ferritin light chain	0.02731654	0.5369199
P11279	Lysosome-associated membrane glycoprotein 1	0.00205766	0.53551125
P49747	Cartilage oligomeric matrix protein	0.00568701	0.52060948
Q7Z7M0	Multiple epidermal growth factor-like domains protein 8	0.01410853	0.51548954
P35443	Thrombospondin-4	0.00611524	0.49246221
O75083	WD repeat-containing protein 1	0.01334526	0.48183401
P62807	Histone H2B type 1-C/E/F/G/I	0.03803625	0.48178598
P18669	Phosphoglycerate mutase 1	0.00761228	0.47797035
P10721	Mast/stem cell growth factor receptor Kit	0.02163147	0.47608593
Q6UXB8	Peptidase inhibitor 16	0.0315392	0.46662679
P27824	Calnexin	0.01495759	0.45917
P00742	Coagulation factor X	0.00012606	0.44927623
P11277	Spectrin beta chain, erythrocytic	0.04755164	0.44927372
P05090	Apolipoprotein D	0.00238571	0.44723834
P00558	Phosphoglycerate kinase 1	0.0016901	0.44552743
P42785	Lysosomal Pro-X carboxypeptidase	0.03667882	0.4255131
P55285	Cadherin-6	0.02915166	0.40098312
P05556	Integrin beta-1	0.0045458	0.38667225
P07911	Uromodulin	0.00549639	0.38614797

Table 6(b) Down-expressed protein in AD in comparison to MI (p<0.05)

P09668	Pro-cathepsin H	0.03331974	0.37683398
P22891	Vitamin K-dependent protein Z	0.02103875	0.37349228
P61981	14-3-3 protein gamma	0.01993608	0.34516782
P03951	Coagulation factor XI	0.00138524	0.33509185
Q5VU43	Myomegalin	0.02503463	0.32715839
P02730	Band 3 anion transport protein	0.00641595	0.28182483
P23141	Liver carboxylesterase 1	0.01159823	0.2637909
P09211	Glutathione S-transferase P	0.00473347	0.23954038
O95897	Noelin-2	0.00502144	0.18324118
P60174	Triosephosphate isomerase	0.00139197	0.16692489
P02144	Myoglobin	0.01930823	0.10235049
P40925	Malate dehydrogenase, cytoplasmic	0.00363283	0.0983941
P06732	Creatine kinase M-type	0.02032649	0.07659113

4.5.4 Functional annotation and enrichment of differential proteins between AD and MI groups

GO and KEGG functional analysis were performed for up-regulated and down-regulated proteins, respectively. GO functional annotation showed that differentially expressed proteins were mainly localized in extracellular regions and vesicles between AD vs MI groups. They are involved in metabolic processes, biological regulation, stimulus response, protein binding, ion binding and other biological functions (Fig.25, Fig.26). KEGG functional analysis showed that the differential proteins between AD and Sham groups were mainly enriched in immune response, cell activation, rabbit disease effector process, cell secretion, cell migration, cell movement, cell adhesion, proteolysis, endoplasmic reticulum, and exocytosis (Fig.27).

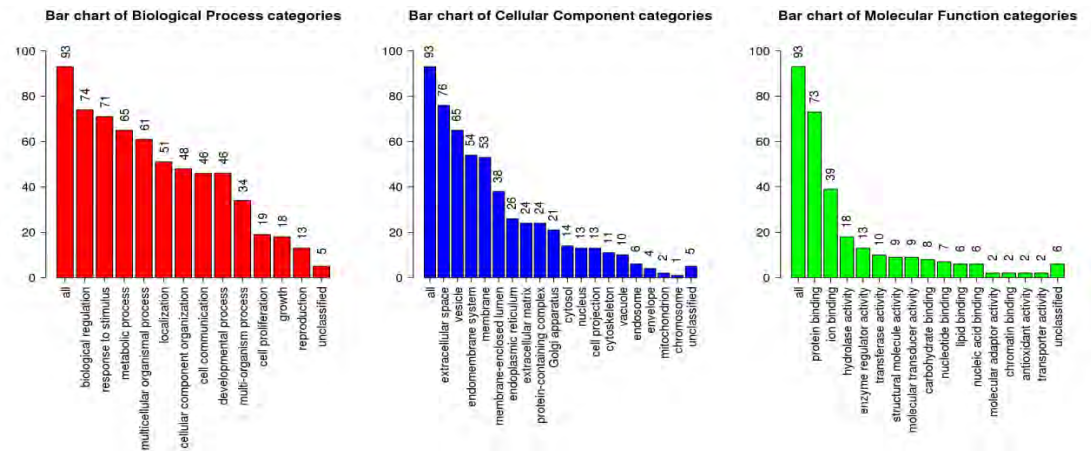

Figure 25: GO Slim summary for up-regulated proteins in AD compared to MI. Each biological Process, cellular component and molecular function category is represented by a red, blue and green bar, respectively. The height of the bar represents the number of IDs in the user list and also in the category.

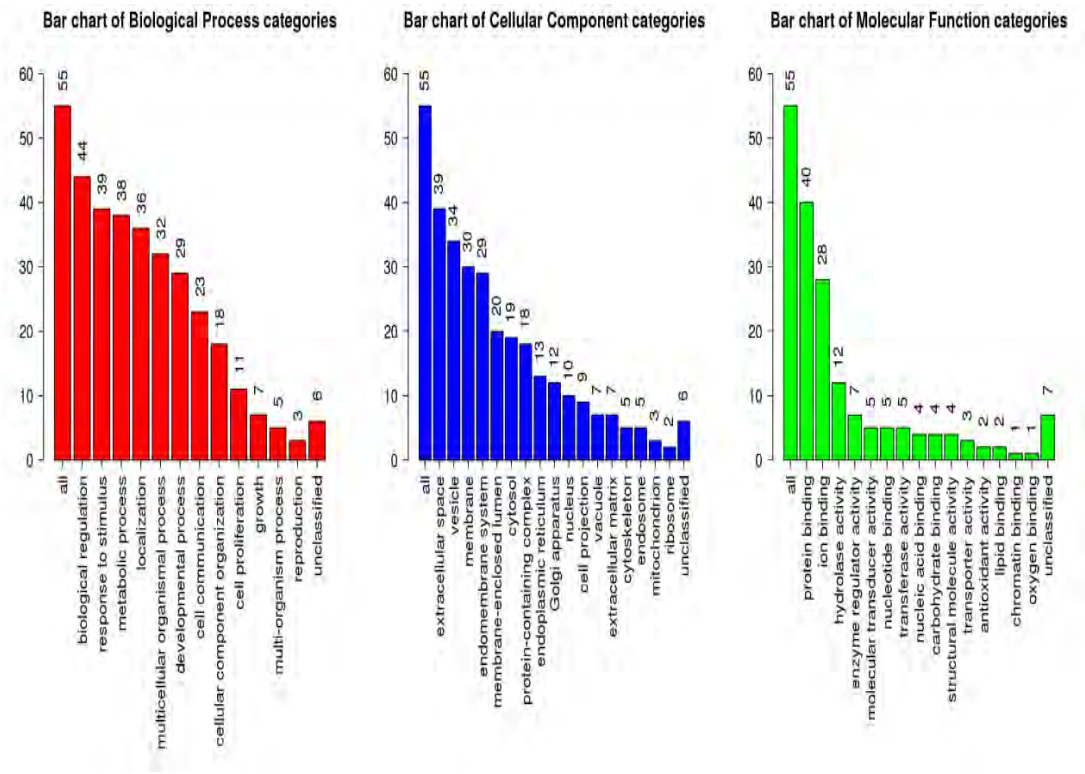

Figure 26: Summary from GO Slim for proteins that are downregulated in AD relative to MI. An individual red, blue, or green bar represents each biological Process, cellular component, and molecular function category. The number of IDs in the category and user lists is indicated by the height of the bar.

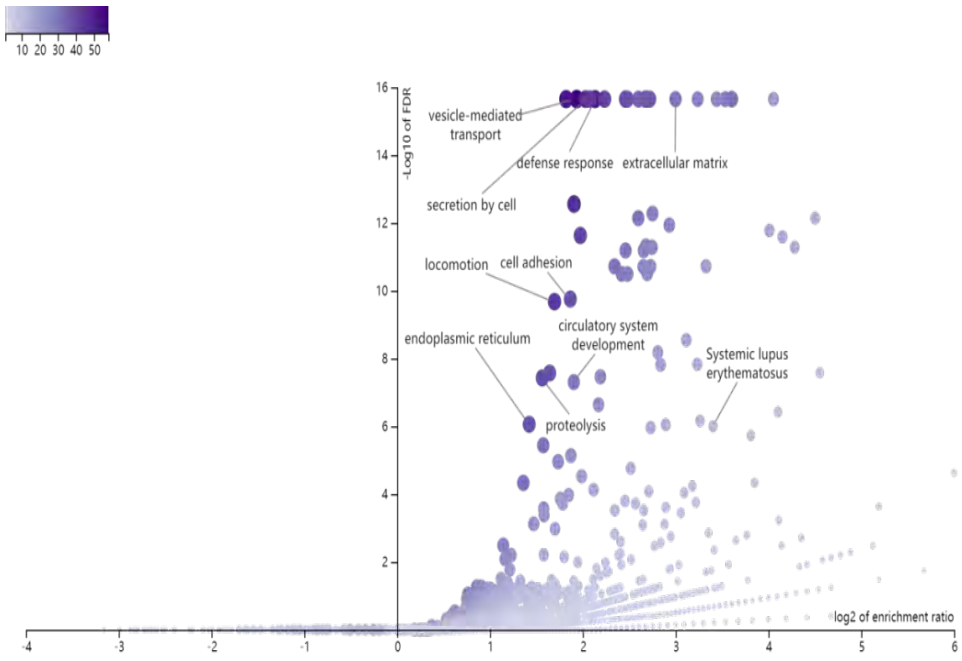

Figure 27: Proteins that were up regulated in AD when compared to MI using the overrepresentation approach are shown in a volcano plot of GO (GOBP, GOCC, and GOMF) and KEGG enrichment results.

5. Verification of differential proteins

5.1 Comparison of relative expression levels of differential proteins and AUC area under ROC curve between MI group and Sham group

In the validation group, the relative expression levels of GALT5, FA11, CNDP1, LV302, RNAS2, GALT2, ATS13, PRAP1 and ALBU proteins in the MI group and the Sham group were significantly different, with statistical significance (P<0.05) (Fig. 28). The AUC areas under the ROC curve of the differential proteins in MI group and Sham group were GALT5 (0.880), FA11 (0.920), CNDP1 (0.840), LV302 (0.960), RNAS2 (1.000), GALT2 (0.960), ATS13 (0.960), P, respectively RAP1 (0.960) and ALBU (0.960) had good diagnostic value (Fig. 29).

Furthermore, the exceptional performance of RNAS2 and GALT2, with AUC values reaching 1.000 and 0.960, respectively, suggests that these proteins may be particularly promising candidates for further development as diagnostic markers. Future research could explore the feasibility of incorporating these proteins into clinical diagnostic tools for improved accuracy and early detection of MI.

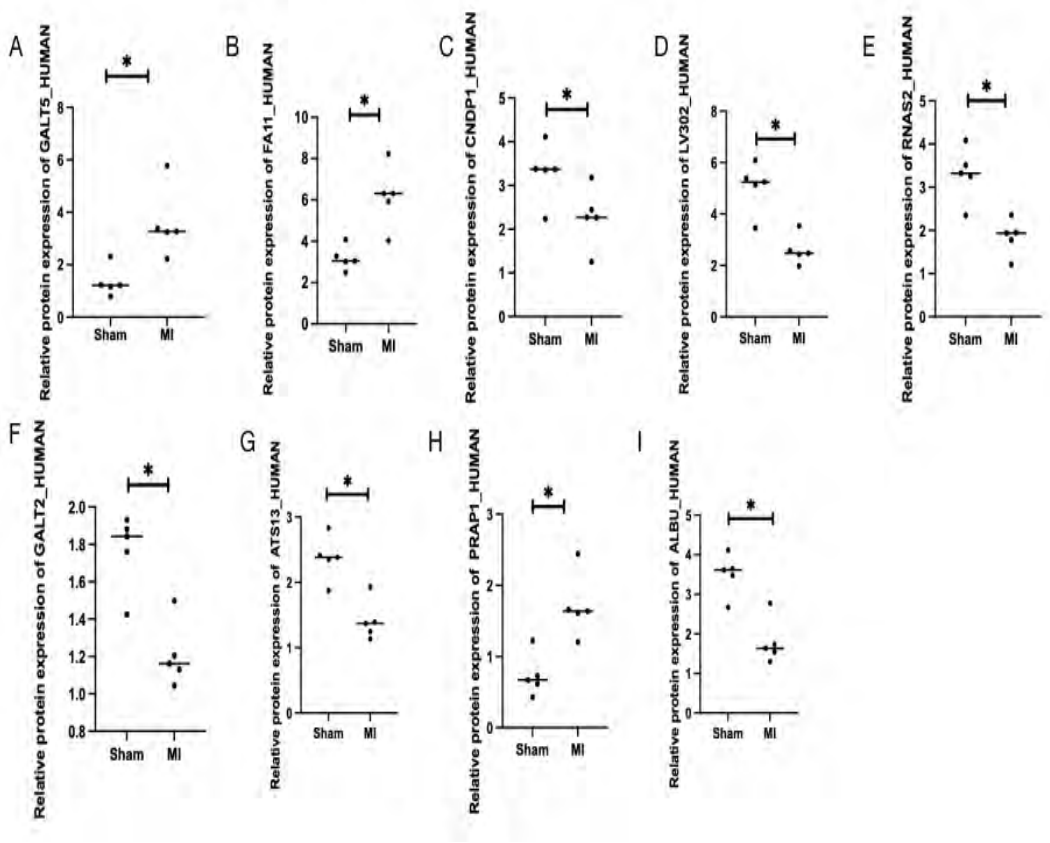

Figure 28 Comparison of relative expression levels of differentially expressed proteins between AMI group and Sham group. A: GALT5; B: FA11; C: CNDP1; D: LV302; E: RNAS2; F: GALT2; G: ATS13; H: PRAP1; I: ALBU. * indicates P<0.05.

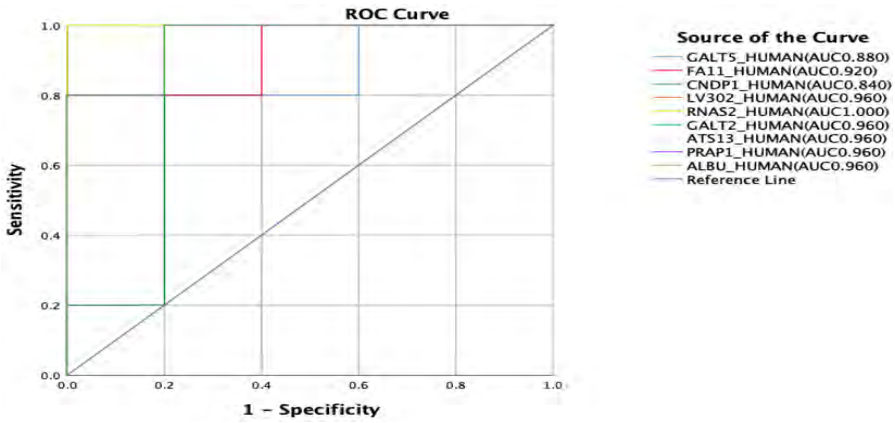

Figure 29: AUC area under the ROC curve of the differential proteins in MI group and Sham group.

5.2 Comparison of relative expression levels of differential proteins and AUC area under ROC curve between AD group and Sham group

In the validation group, the relative expressions of CNDP1, PROC, CSPG2, FA7, CAD11, SAA1, GPV, KIT, and ASGR2 proteins in the AD group and Sham group were significantly different, with statistical significance (P<0.05) (Fig. 30). Verify the AD group and Sham group. The AUC areas under the ROC curve of the differential proteins were CNDP1 (0.960), PROC (0.960), CSPG2 (0.920), FA7 (0.960), CAD11 (0.960), SAA1 (0.960), GPV (1.000), KIT (1.000) and ASGR, respectively 2 (0.920), which had good diagnostic value (Fig. 31).

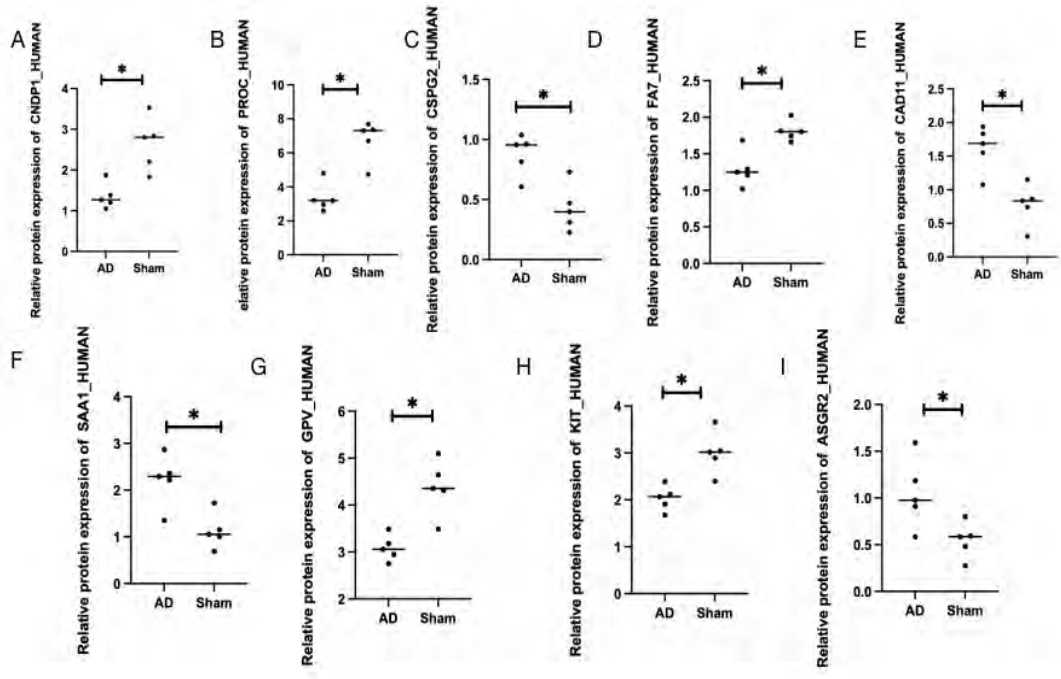

Figure 30: Comparison of the relative expression levels of differential proteins between the AD group and the Sham group. A: CNDP1; B: PROC; C: CSPG2; D: FA7; E: CAD11; F: SAA1; G: GPV; H: KIT; I: ASGR2. * indicates P<0.05.

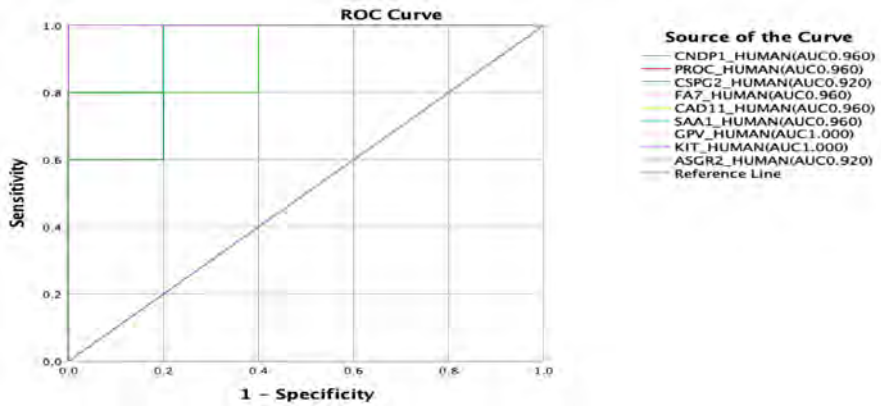

Figure 31 AUC area under ROC curve of differential proteins in AD group and Sham group.

5.3 Comparison of differential protein relative expression and AUC area under ROC curve between AD group and MI group

In the validation group, the relative expressions of SAA1, ASGR2, GALT5, FA10, CO6, FA7, TENA, FA11, TPIS, and IBP4 proteins in the AD group and the MI group were significantly different, with statistical significance ($P < 0.05$) (Figure 32). Notably, these proteins exhibited distinct expression patterns in the two groups, suggesting their potential involvement in the underlying biological mechanisms of both AD and MI. Furthermore, the AUC area under the ROC curve of these proteins demonstrated their strong diagnostic value in differentiating AD and MI athletic patients. As shown in Figure 33, all ten proteins displayed AUC values exceeding 0.8, with several exceeding 0.960. This indicates their high accuracy and potential utility as reliable biomarkers for diagnosis. These findings warrant further investigation to validate their clinical applicability and explore their therapeutic potential.

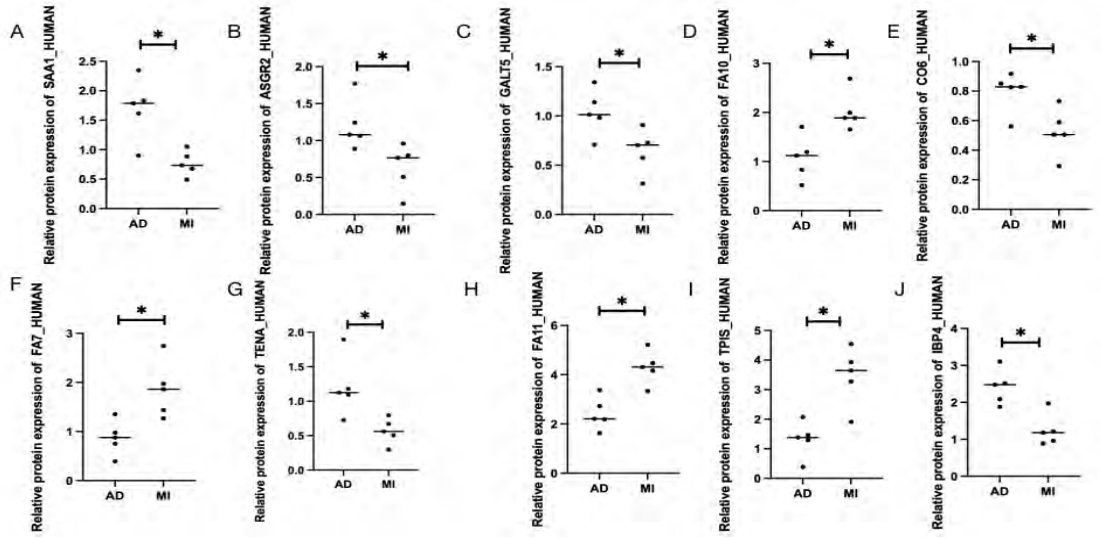

Figure 32: Comparison of the relative expression levels of differentially expressed proteins between the AD group and the MI group. A: SAA1; B: ASGR2; C: GALT5; D: FA10; E:CO6; F: FA7; G: TENA; H: FA11; I: TPIS; J: IBP4. * indicates $P<0.05$.

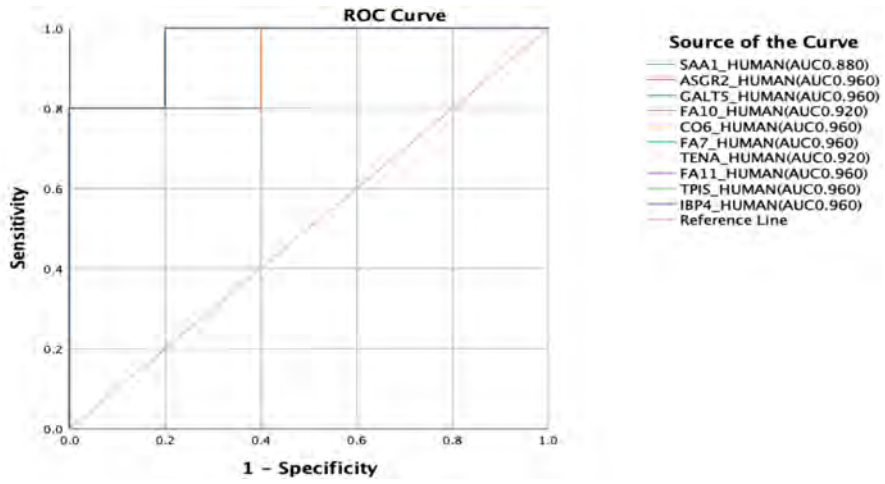

Figure 33: AUC area under ROC curve of differential proteins in AD group and MI group.

6. Discussion

Aortic dissection complicated with AMI is often misdiagnosed as AMI, which also leads to the serious life threat of athletic patients. Proteomics by high throughput, high sensitive technology with different types or different sample of all proteins on a large scale, the panorama of quantitative analysis and comparison, contrast protein expression differences between samples or sample of the exact content of protein, proteomics can from different aspects to reveal the law of life activities (Midha et al., 2020). In recent years, DIA technology has shown broad application prospects in the study of disease prevention, disease diagnosis, treatment monitoring and prognosis assessment (Krasny & Huang, 2021).

There were no statistically significant differences in age, sex, BMI, or blood pressure among the subjects collected in this survey, and follow-up experiments could be carried out. In this study, we analyzed serum samples from three groups of athletic patients by proteomic DIA technology. Finally, 1063 proteins were quantified in 15 samples. Each sample could be quantified to nearly 900 proteins, and the dynamic intensity range of these proteins was more than 6 orders of magnitude. It shows that the unlabeled quantification method based on DIA can achieve the deep coverage of serum proteome, which provides a strong guarantee for the subsequent in-depth analysis of the changes of serum proteome among different groups. After missing value processing, protein molecules with a proportion of missing value greater than 40% in any group were removed, and KNN algorithm was used to fill in the data set filtered by missing value. After processing, 769 proteins were used for statistical analysis. PCA analysis showed significant differences between the two groups of proteomes, and the model was effective and robust with good predictive ability. The quantitative protein results of the two groups were analyzed by t-test, and the differentially expressed proteins between each two groups were screened with $P < 0.05$ as the threshold. The differentially

expressed proteins were primarily found in vesicles and extracellular space, according to GO and KEGG functional analyses, which were involved in biological regulation, stimulation response, metabolic processes, processes of multicellular organisms, protein binding, ion binding, hydrolase activity and other biological functions. KEGG function analysis showed that the differentially expressed proteins between MI vs Sham groups were mainly enriched in vesicle-mediated transport, immune response, cell secretion, cytoplasmic vesicle fraction, cell activation, proteolysis, secretory granules, exocytosis, regulation of exocytosis, and leukocyte mediated immunity. Extracellular proteins are secreted proteins, which are synthesized in cells and transported to the outside of cells through membranes and vesicles to play physiological functions. Secreted proteins not only participate in immune response, signal transduction and other biological processes in life activities, but also play an important role in inflammatory diseases (Liu, Cai, & Wang, 2021). In addition, these differential proteins are also involved in biological processes such as cellular processes, stimulation responses, immune responses, adhesion, catalytic activity and molecular conversion activity. These biological mechanisms may be crucial in AD and AMI.

As mentioned above, there are hundreds of differentially expressed proteins in the AD and MI groups, and these differentially expressed proteins are involved in multiple biological processes and play dozens of molecular functions. However, due to the large number of differentially expressed proteins between groups, it is not possible to verify and evaluate the diagnostic value of AD and AMI. Therefore, in this study, after a series of screening, the differential proteins between MI group and Sham group were finally obtained: GALT5, FA11, CNDP1, LV302, RNAS2, GALT2, ATS13, PRAP1, ALBU. The differential proteins between AD group and Sham group: CNDP1, PROC, CSPG2, FA7, CAD11, SAA1, GPV, KIT, ASGR2; The differentially expressed proteins in AD group and MI group were SAA1, ASGR2, GALT5, FA10, CO6, FA7, TENA, FA11, TPIS and IBP4. The relative expression levels of the above proteins were determined by Westem Blot analysis in the validation group. The results showed that the relative expression levels of each protein were significantly different between the two groups, and the AUC area under the ROC curve of the different proteins was large, which had high diagnostic value. Therefore, this study speculated that SAA1, ASGR2, GALT5, FA10, CO6, FA7, TENA, FA11, TPIS and IBP4 may be potential markers for the diagnosis and differential diagnosis of AD and AMI.

Studies have found that AD is a large vascular disease associated with inflammation, which plays a key role in a series of pathological changes such as vascular smooth muscle cell (VSMC) necrosis, apoptosis and vascular elastic structural degeneration, and eventually leads to aortic aneurysm rupture or dissection (Matsuo et al., 2021). Serum amyloid A1 (SAA1) is an apolipoprotein of high-density lipoprotein cholesterol (HDL-C), which is mostly

contributes to the acute inflammatory response and represents the body's inflammatory state. It performs a variety of tasks in cardiovascular disorders, including controlling the aorta's MMP activity and triggering systemic inflammatory response (Zhu et al., 2019). SAA1 participates in MAPK signaling pathway, induces phosphorylation of p38, promotes differentiation of Th17 cells, and releases pro-inflammatory cytokines, which trigger immune disorders and amplify inflammatory reactions in circulation and blood vessels, leading to VSMC injury, vascular remodeling and dilation, and eventually lead to AD and dissection rupture (Beekman-van Solkema, Schoots, & Pundziute-Do Prado, 2020). GATA5 is a crucial member of the GATA family that plays a crucial part in the onset and progression of cardiovascular illnesses include congenital heart disease, atrial fibrillation, and hypertension (Singh, Kayal, & Nath, 2021), which may be related to the occurrence of AD. IBP4 is an anti-angiogenic factor, which is related to the occurrence of heart failure (Benbouchta, Berrajaa, Ofkire, El Ouafi, & Bazid, 2020). FA10, FA7 and FA11 are all coagulation factors, and the level of FA10 (coagulation factor X) plays a great role in the coagulation function of athletic patients with aortic dissection during the perioperative period(Haruta & Arai, 2020). The low level of FA10 at the lowest temperature during the operation may be an independent risk factor for postoperative secondary thoracotomy due to coagulation dysfunction. Coagulation factor X is an important factor in the common coagulation pathway (Forrer et al., 2021).

7. Conclusion

In conclusion, this study emphasizes the potential of serum DIA as a valuable diagnostic tool for identifying aortic dissection (AD) and acute myocardial infarction (AMI) in athletic patients. The differential protein profiles revealed by DIA technology provide a deeper understanding of the unique cardiovascular risks faced by athletes. This research not only broadens our knowledge of biomarkers in cardiovascular conditions but also opens new avenues for targeted diagnostic approaches in athletic populations, enhancing early detection and management of these critical conditions.

Funding Statement

Social Development Foundation of ZhenJiang City (SH2020028，SH2019048) and Jinshan Medical Talents Plan of ZhenJiang City(2021-JSYZ-4)

Reference

Beekman-van Solkema, G., Schoots, M., & Pundziute-Do Prado, G. (2020). A rare cause of acute ST-elevation myocardial infarction: case report of native aortic valve thrombosis. *European Heart Journal: Case Reports, 4*(1), 1.

Benbouchta, K., Berrajaa, M., Ofkire, M., El Ouafi, N., & Bazid, Z. (2020). An

uncommon acute type A aortic dissection mimicking an inferior STEMI. *Pan African Medical Journal, 36*(1).

Chen, H.-Y., Lu, D.-Y., & Sung, S.-H. (2019). Acute myocardial infarction and coronary intramural haematoma: a clue to aortic dissection. *Eurointervention: Journal of Europcr in Collaboration with the Working Group on Interventional Cardiology of the European Society of Cardiology, 14*(18), e1852-e1853.

Cui, H., Chen, Y., Li, K., Zhan, R., Zhao, M., Xu, Y., . . . Tang, P. C. (2021). Untargeted metabolomics identifies succinate as a biomarker and therapeutic target in aortic aneurysm and dissection. *European Heart Journal, 42*(42), 4373-4385.

Farmer, N., Rushmer, T., Wykes, J., & Mallmann, G. (2020). The Macquarie Deformation-DIA facility at the Australian Synchrotron: A tool for high-pressure, high-temperature experiments with synchrotron radiation. *Review of scientific instruments, 91*(11).

Forrer, A., Schoenrath, F., Torzewski, M., Schmid, J., Franke, U. F., Göbel, N., . . . Mach, F. (2021). Novel blood biomarkers for a diagnostic workup of acute aortic dissection. *Diagnostics, 11*(4), 615.

Haruta, S., & Arai, K. (2020). Acute myocardial infarction caused by coronary spasm and dissection treated with medical therapy. *International Heart Journal, 61*(1), 169-173.

Hussain, A., Rossi, A., Smith, A., Lopez-Marco, A., Khalil, A., & Roberts, N. (2021). Type A Aortic Dissection Masquerading as an Inferior Myocardial Infarction. *AORTA, 9*(05), 184-185.

Karayel, O., Michaelis, A. C., Mann, M., Schulman, B. A., & Langlois, C. R. (2020). DIA-based systems biology approach unveils E3 ubiquitin ligase-dependent responses to a metabolic shift. *Proceedings of the National Academy of Sciences, 117*(51), 32806-32815.

König, K. C., Lahm, H., Dreßen, M., Doppler, S. A., Eichhorn, S., Beck, N., . . . Kastrati, A. (2021). Aggrecan: a new biomarker for acute type A aortic dissection. *Scientific reports, 11*(1), 10371.

Krasny, L., & Huang, P. H. (2021). Data-independent acquisition mass spectrometry (DIA-MS) for proteomic applications in oncology. *Molecular omics, 17*(1), 29-42.

Li, K. W., Gonzalez-Lozano, M. A., Koopmans, F., & Smit, A. B. (2020). Recent developments in data independent acquisition (DIA) mass spectrometry: application of quantitative analysis of the brain proteome. *Frontiers in molecular neuroscience, 13*, 564446.

Liu, B., Cai, L.-D., & Wang, Y. (2021). Association between delayed transthoracic echocardiography and in-hospital mortality in type A acute aortic dissection-associated ST-segment elevated myocardial infarction. *Journal of thoracic disease, 13*(5), 2923.

Liu, F., Qian, S.-C., Jing, S., Wang, Z., Yang, X.-C., & Chen, M.-L. (2021). Incidence and outcome of acute myocardial infarction in patients with

aortic dissection and risk factor control. *Frontiers in Surgery, 8*, 678806.

Matsuo, Y., Ozaki, K., Ikegami, R., Nishida, K., Kubota, N., Takano, T., . . . Kashimura, T. (2021). Conservative treatment with an intra-aortic balloon pump to treat acute myocardial infarction due to spontaneous coronary artery dissection. *Journal of Cardiology Cases, 23*(6), 274-280.

Midha, M. K., Kusebauch, U., Shteynberg, D., Kapil, C., Bader, S. L., Reddy, P. J., . . . Moritz, R. L. (2020). A comprehensive spectral assay library to quantify the Escherichia coli proteome by DIA/SWATH-MS. *Scientific data, 7*(1), 389.

Quan, J., Kang, Y., Li, L., Zhao, G., Sun, J., & Liu, Z. (2021). Proteome analysis of rainbow trout (Oncorhynchus mykiss) liver responses to chronic heat stress using DIA/SWATH. *Journal of Proteomics, 233*, 104079.

Singh, A. P., Kayal, V., & Nath, R. K. (2021). Aortic Dissection With Complete Occlusion of Left Main Coronary Artery Presenting as Acute ST-Segment Elevation Myocardial Infarction. *Cureus, 13*(6).

Usami, K., Sai, S., & Ieda, M. (2021). Acute myocardial infarction caused by aortic dissection manifesting as mobile mass in ascending aorta: a case report. *European Heart Journal-Case Reports, 5*(7), ytab241.

Wang, W., Wu, J., Zhao, X., You, B., & Li, C. (2019). Type-A aortic dissection manifesting as acute inferior myocardial infarction: 2 case reports. *Medicine, 98*(43).

Zhang, Y.-X., Yang, H., & Wang, G.-S. (2021). Acute inferior wall myocardial infarction induced by aortic dissection in a young adult with Marfan syndrome: A case report. *World Journal of Clinical Cases, 9*(4), 970.

Zhu, S., Zheng, T., Qiao, Z.-Y., Chen, L., Ou, J.-F., Fang, W.-G., . . . Zheng, J. (2019). Acute aortic dissection in young adult patients: clinical characteristics, management, and perioperative outcomes. *Journal of Investigative Surgery*.

Zlatanovic, P., Dragas, M., Cvetkovic, S., Dimic, A., Mitrovic, A., Vujcic, A., . . . Davidovic, L. (2021). Open surgical treatment of acute spontaneous isolated abdominal aortic dissection. *Annals of Vascular Surgery, 74*, 525. e513-525. e521.